

Recent Activities Related to Nuclear Data Evaluation and Calculations in China

Sun Weili

**Institute of Applied Physics and Computational
Mathematics Beijing 100088, China**

China Nucl. Data Committee



China Nucl. Data Center

↔ Network



Evaluation

Benchmark

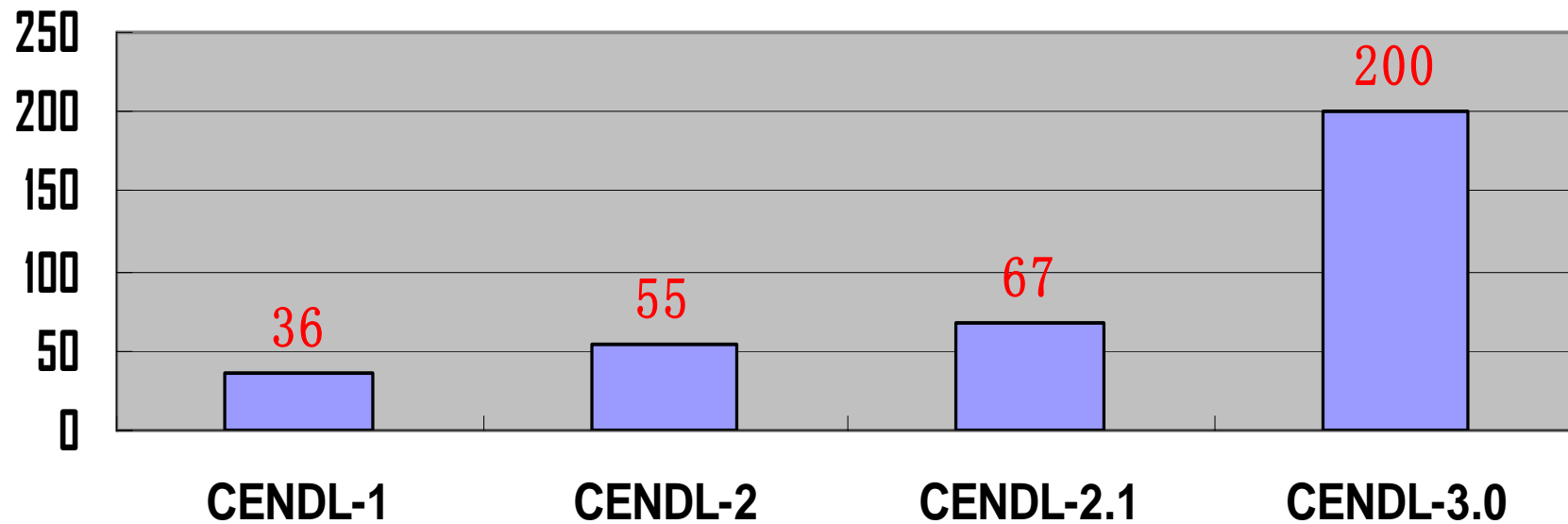
Measurement

Sichuan U.
Lan Zhou U.
Tsing Hua U.
Nan Kai U.
IAPCM

.....

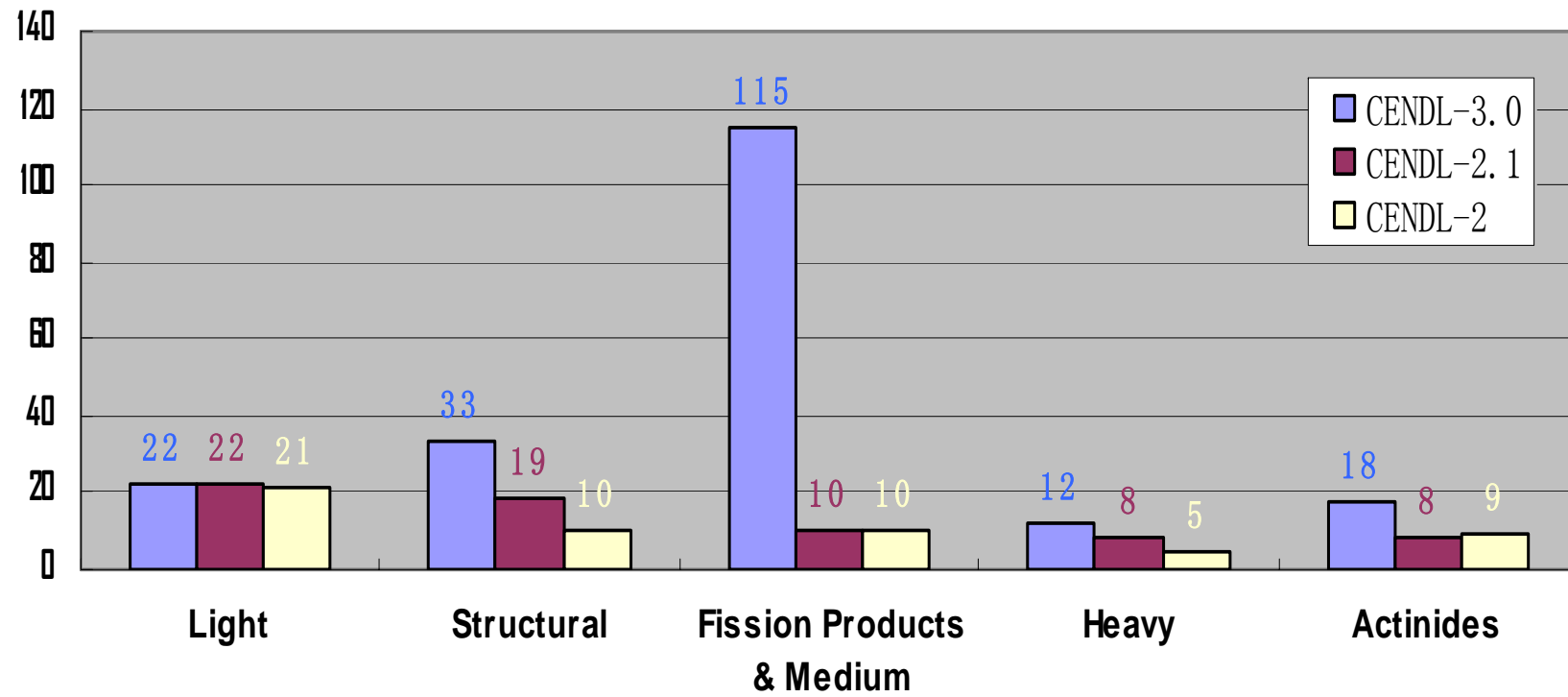
Chinese Evaluated Nuclear Data Library (CENDL)

No. of Nuclides of CENDL



1995--2000

CONTENT OF CENDL- 3.0



Nucl.	Content
Light Elements	1,2,3H, 3,4He, 6,7Li, 9Be, 10,11B, 12C, 14N, 16O, 19F, 23Na, natMg, 27Al, natSi, 31P, natS, natCl, natK, natCa
Structural Materials	natTi, natV, 50,52,53,54, natCr, 55Mn, 54,56,57,58, natFe, 59Co, 58,60,61,62,64, natNi, 63,65, natCu, natZn
Fission Products & Medium Elements	69,71, natGa, 83,84,85,86Kr, 85,87, natRb, 88,89,90Sr, 89,91Y, 90,91,92,93,94, 95,96, natZr, 93,95Nb, 95,97,98,100, natMo, 99Tc, 99,100,101,102,103,104,105Ru, 103Rh, 105,108Pd, 107,109, natAg, 113, natCd, 115, natIn, natSn, 121,123, natSb, 130Te, 127I, 124,129,131,132,134,135,136Xe, 133,134,135,137Cs, 130,132,134,135,136,137,138, natBa, 139La, 140,141,142,144Ce, 141Pr, 142,143,144,145,146,147,148,150, natNd, 147,148,149Pm, 144,147,148,149,150,151,152,154, natSm, 151,153,154,155, natEu, 152,154,155,156,157,158,160, natGd, 164Dy
Heavy Elements	natLu, natHf, 181Ta, natW, 197Au, natHg, natTl, 204,206,207,207, natPb,
Actinides	233,234,235,236,238,239U, 237Np, 238,239,240,241,242Pu, 241,242Am, 249Bk, 249Cf

Table 1. The Nuclides of CENDL-3.1 (>300)

1. Covariance study

Code:

EXPOV: Covariance Matrix for exp. data

SPC : Spline fitting

58,60,61,62,64,natNi, 63,65,natCu, ²⁷Al

RAC : R matrix theory for light nuclide

6, ⁷Li, ¹⁰, ¹¹B, ¹⁶O

2. Data file for ADS

Code: MEND

- **Neutron: 20 -- 250MeV**

50,52,53,54Cr, 54,56,57,58Fe, 90,91,92,94,96Zr,
180,182,183,184,186W, 204,206,207,208Pb, 238U.

- **Proton: thresholds – 250MeV**

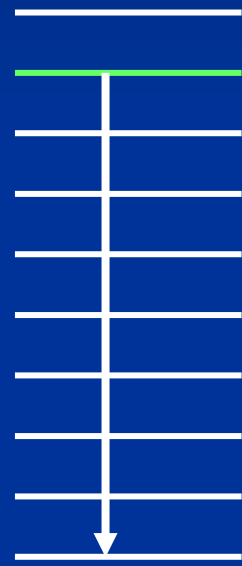
54,56,57,58Fe, 180,182,183,184,186W,
204,206,207,208Pb, 209Bi, 238U.

3. Calculation for Light Nuclei Reaction ($< 20 \text{ MeV}$)

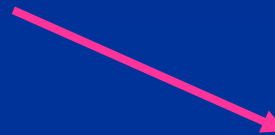
$n + A$



$(A+1)^*$

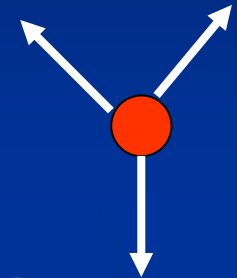


$R1^*$



$R2^*$

multi-particle
recoil effect
3-body Break-up



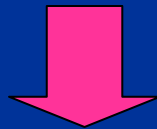
Methods

- **Unified Hauser-Feshbach and Exciton model**

Zhang J. S et al, NSE. 114 (1993) 55

2- body process;
multi-particle emission;
kinematics & dynamics;

3-body break-up process;
recoil effect;



- **Model theory for light nuclei**

Zhang J. S. et al, NSE. 133 (1999) 218

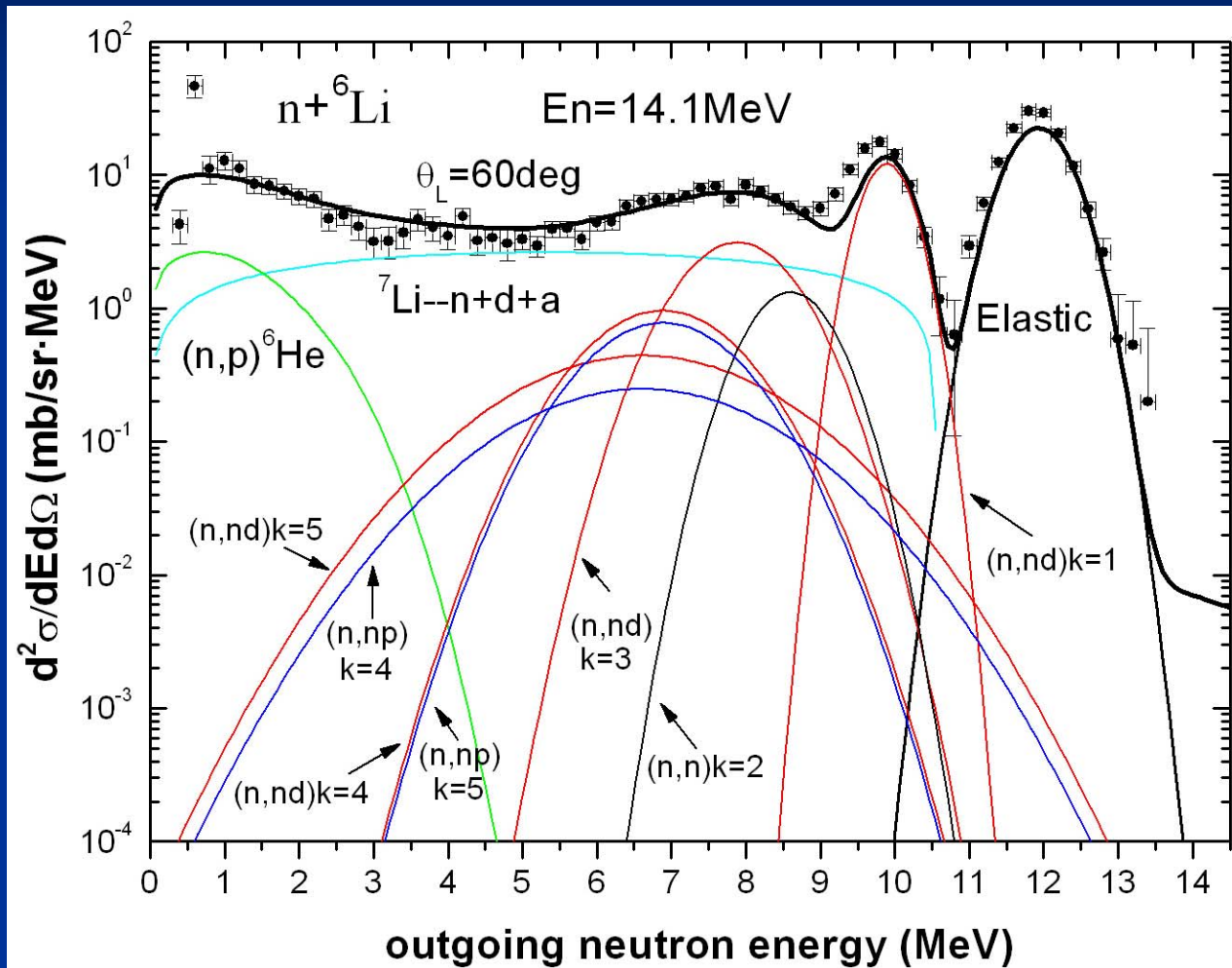
Data file (CENDL-3.1)

- ${}^6\text{Li}$, ${}^7\text{Li}$, ${}^9\text{Be}$, ${}^{10}\text{B}$, ${}^{11}\text{B}$, ${}^{12}\text{C}$, ${}^{16}\text{O}$, ${}^{19}\text{F}$
(1 p-shell)

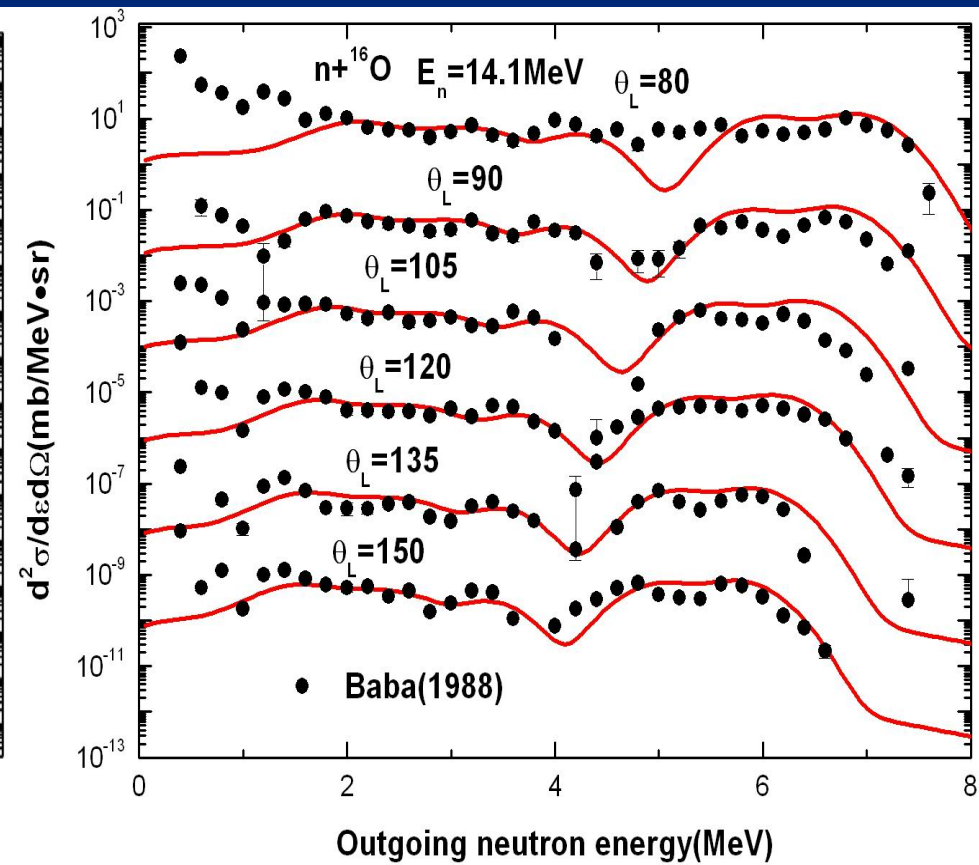
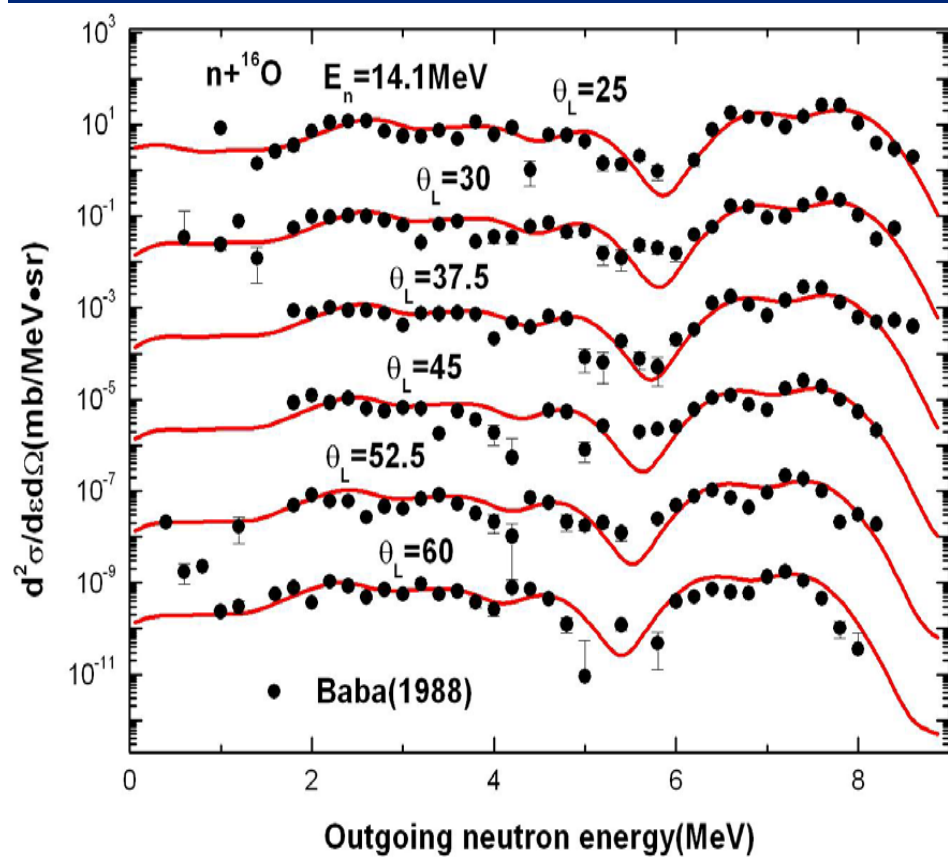
Particularly, File 6 (DDX for all emitted particles) is established, where the energy balance is strictly considered.

Code: LUNF

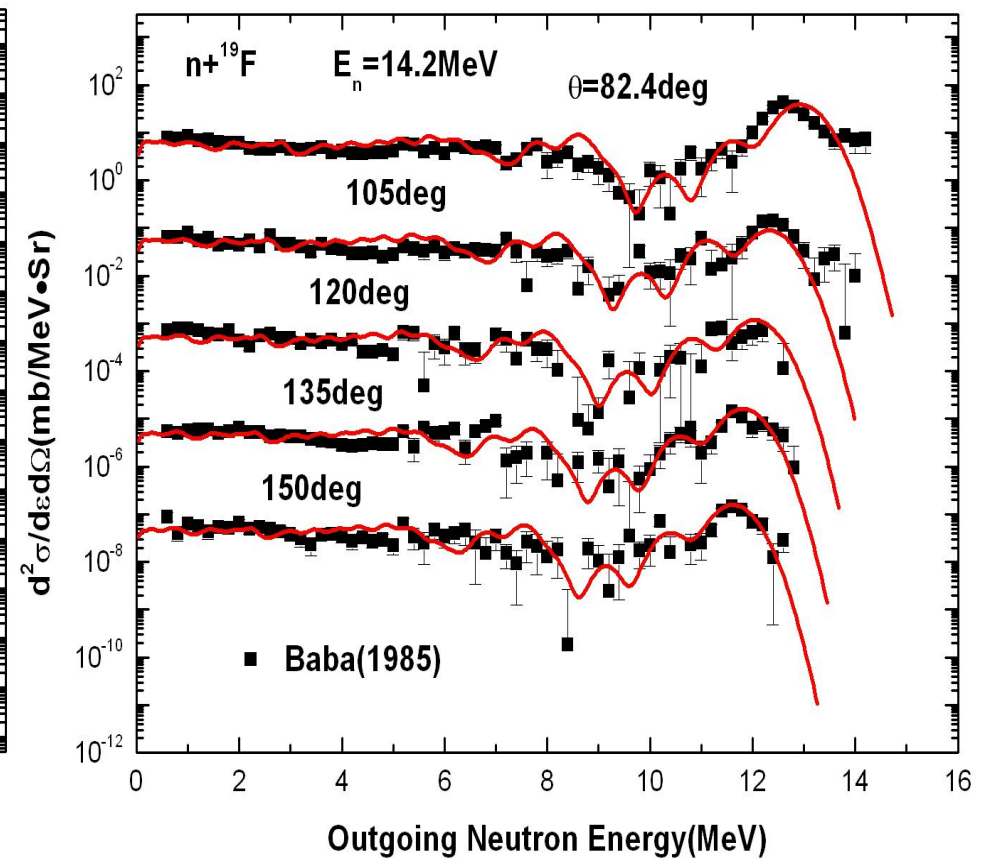
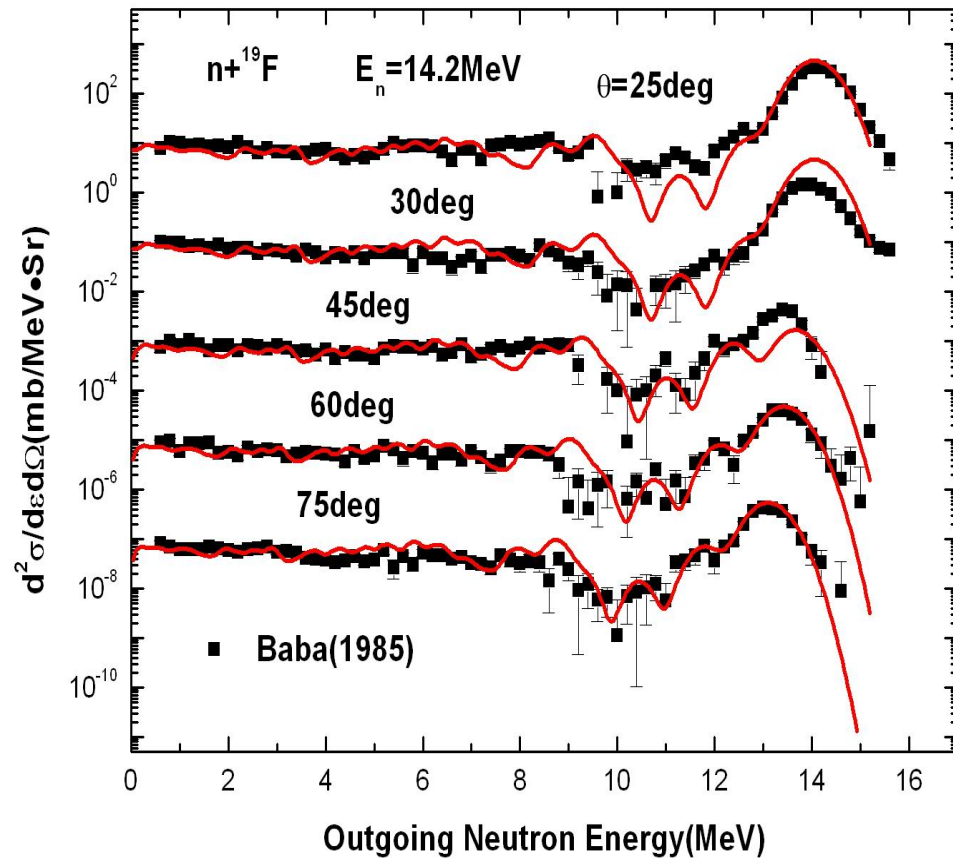
$n + {}^6\text{Li}$ Neutron DDX



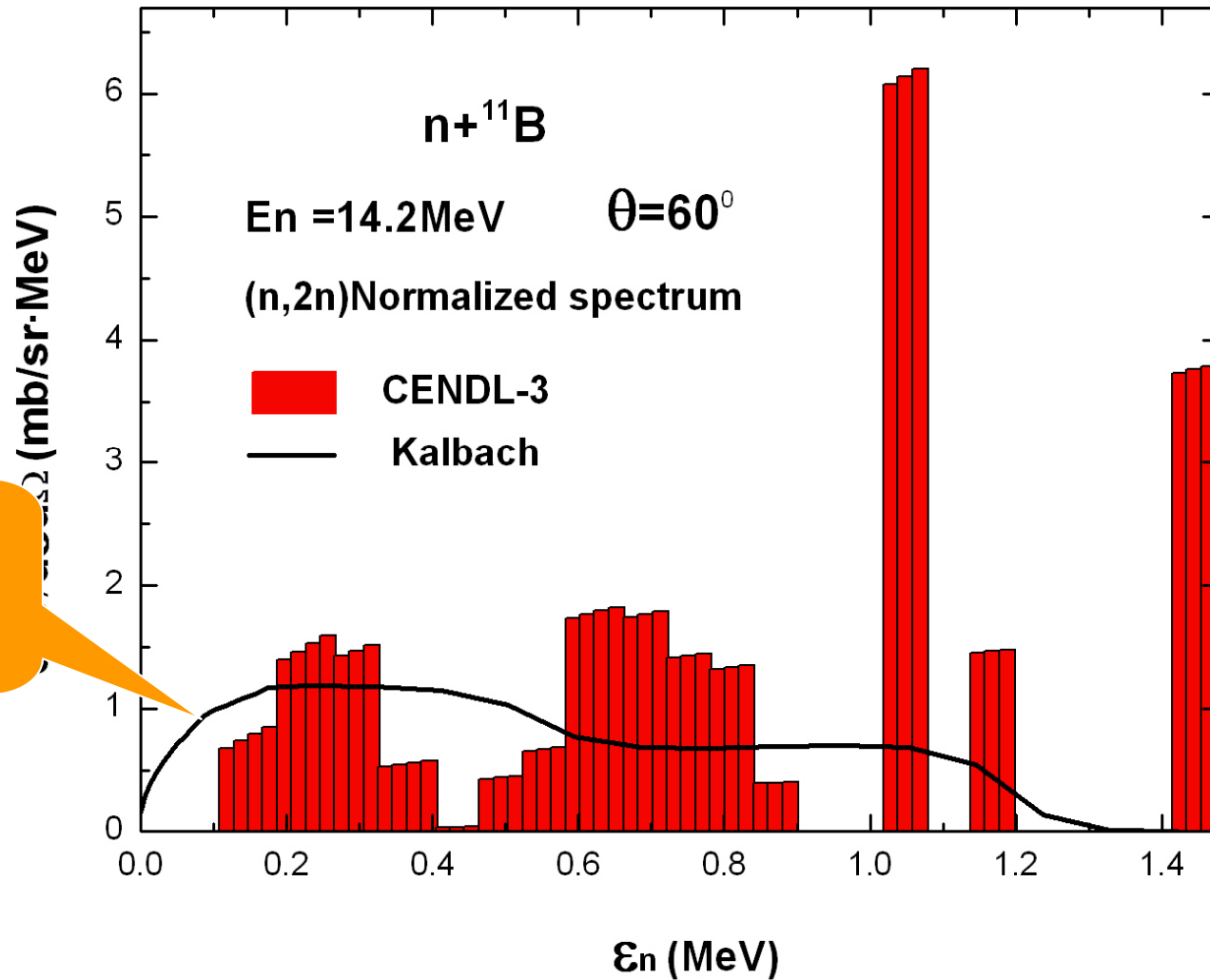
$n + {}^{16}\text{O}$ Neutron DDX



$n + {}^{19}\text{F}$ Neutron DDX

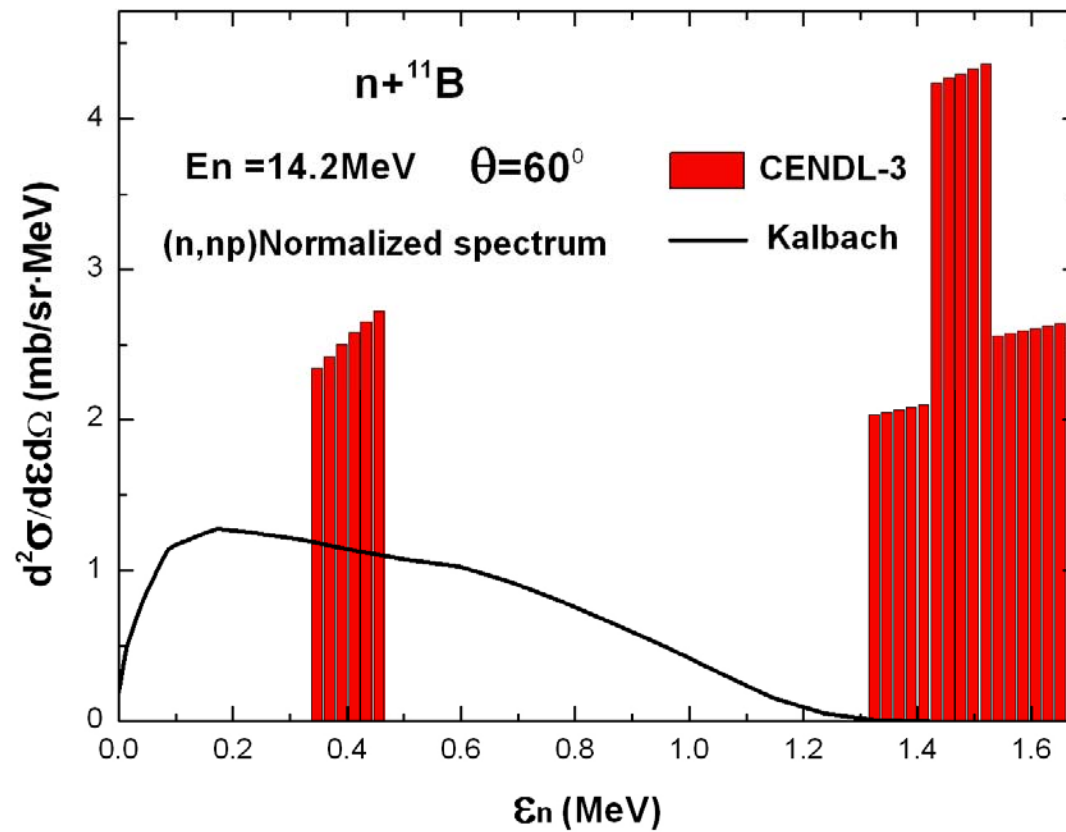


Energy Spectra of (n, 2n) reaction

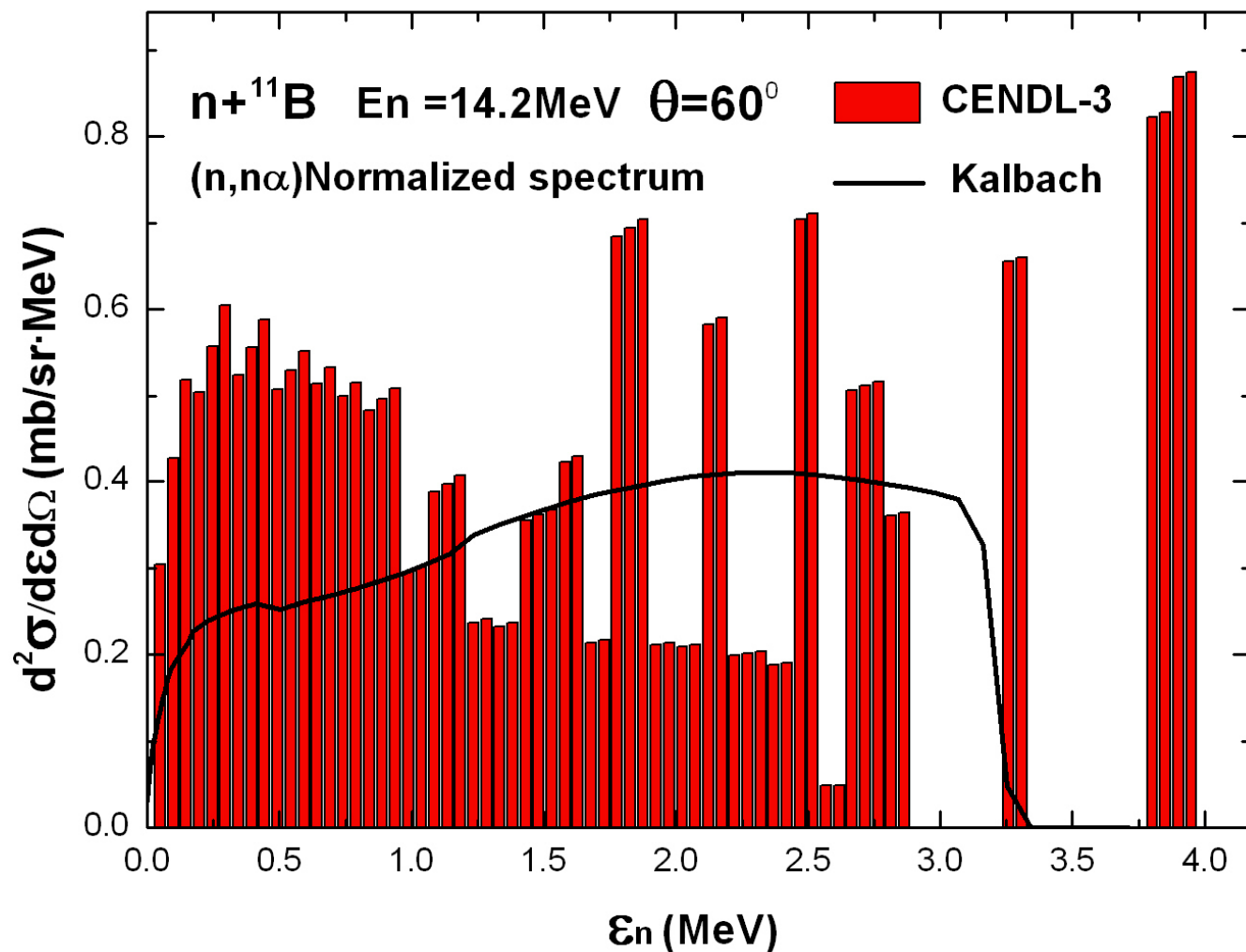


ENDF
/B6.8

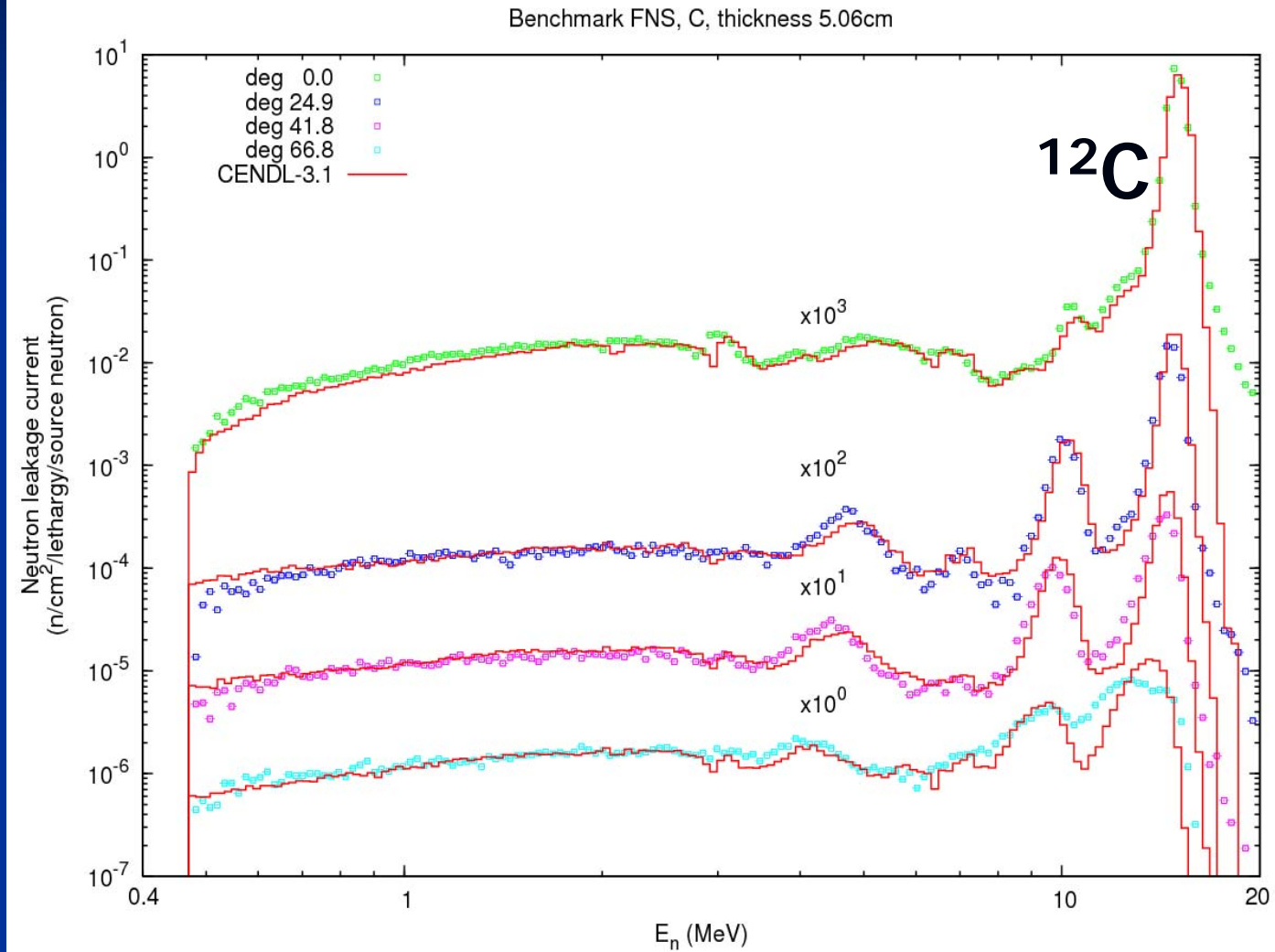
Spectra of $^{11}\text{B}(n, np)$ reaction



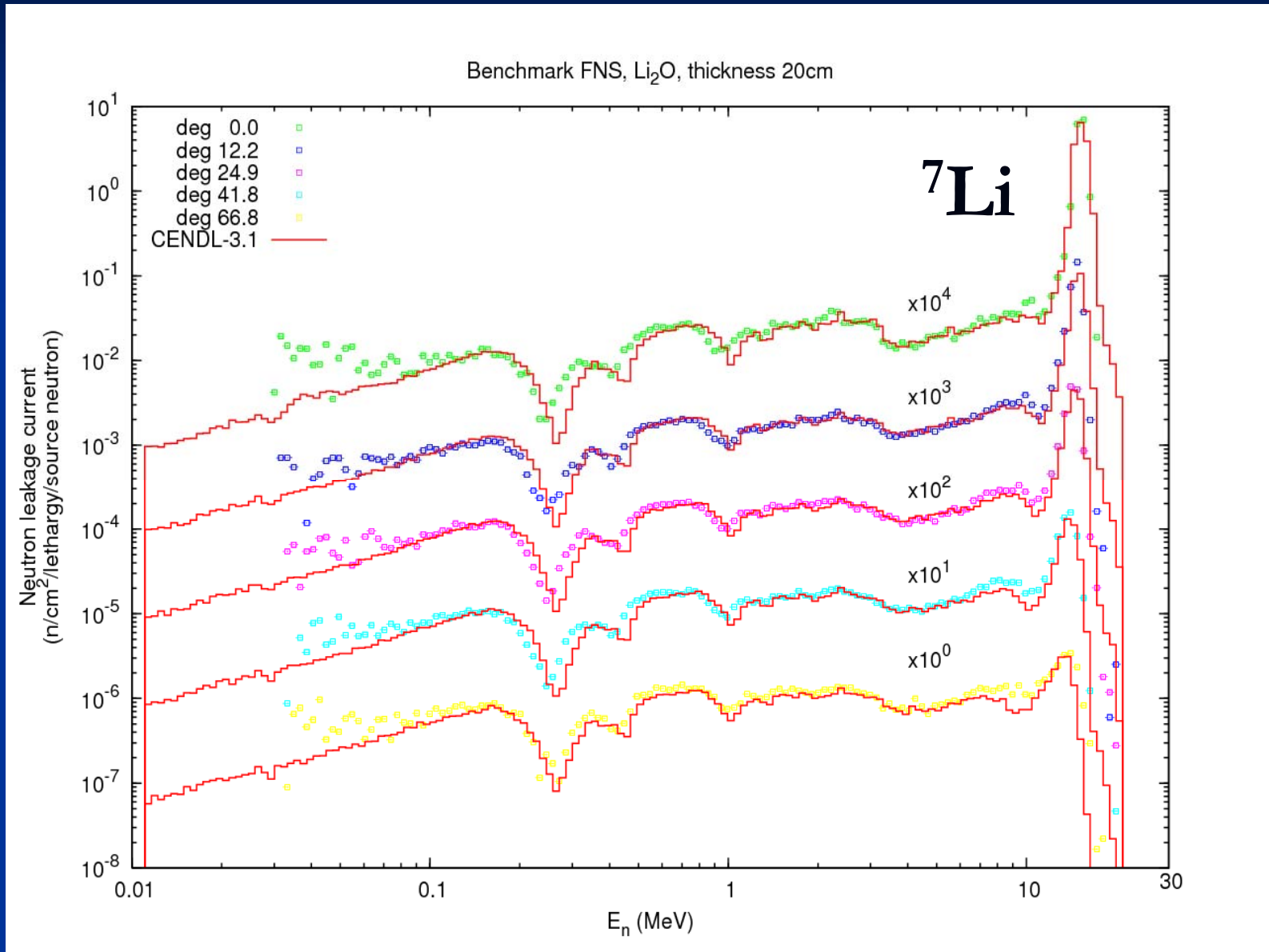
Energy Spectra of $^{11}\text{B}(n, n \alpha)$ reaction



Neutron spectrum for the FNS C



Neutron spectrum for the FNS LiO2



^5He emission

- Generally, n, p, d, t, ^3He , ^4He emission
- ^5He emission, possibility ?

Experimentally,

Turk et al. Nucl. Phys.A431(1984) 31

Theoretically,

Zhang J.S. Sci. in China Ser.
G. Phy. 47 (2004) 137

Threshold
 ${}^3\text{He}$ vs ${}^5\text{He}$



核素	${}^3\text{He}$	${}^5\text{He}$
${}^9\text{Be}$	24.04	3.74
${}^{10}\text{B}$	17.34	5.89
${}^{11}\text{B}$	25.27	10.43
${}^{12}\text{C}$	21.1	8.95
${}^{14}\text{N}$	18.62	13.41
${}^{16}\text{O}$	15.64	8.56
${}^{19}\text{F}$	17.08	5.17

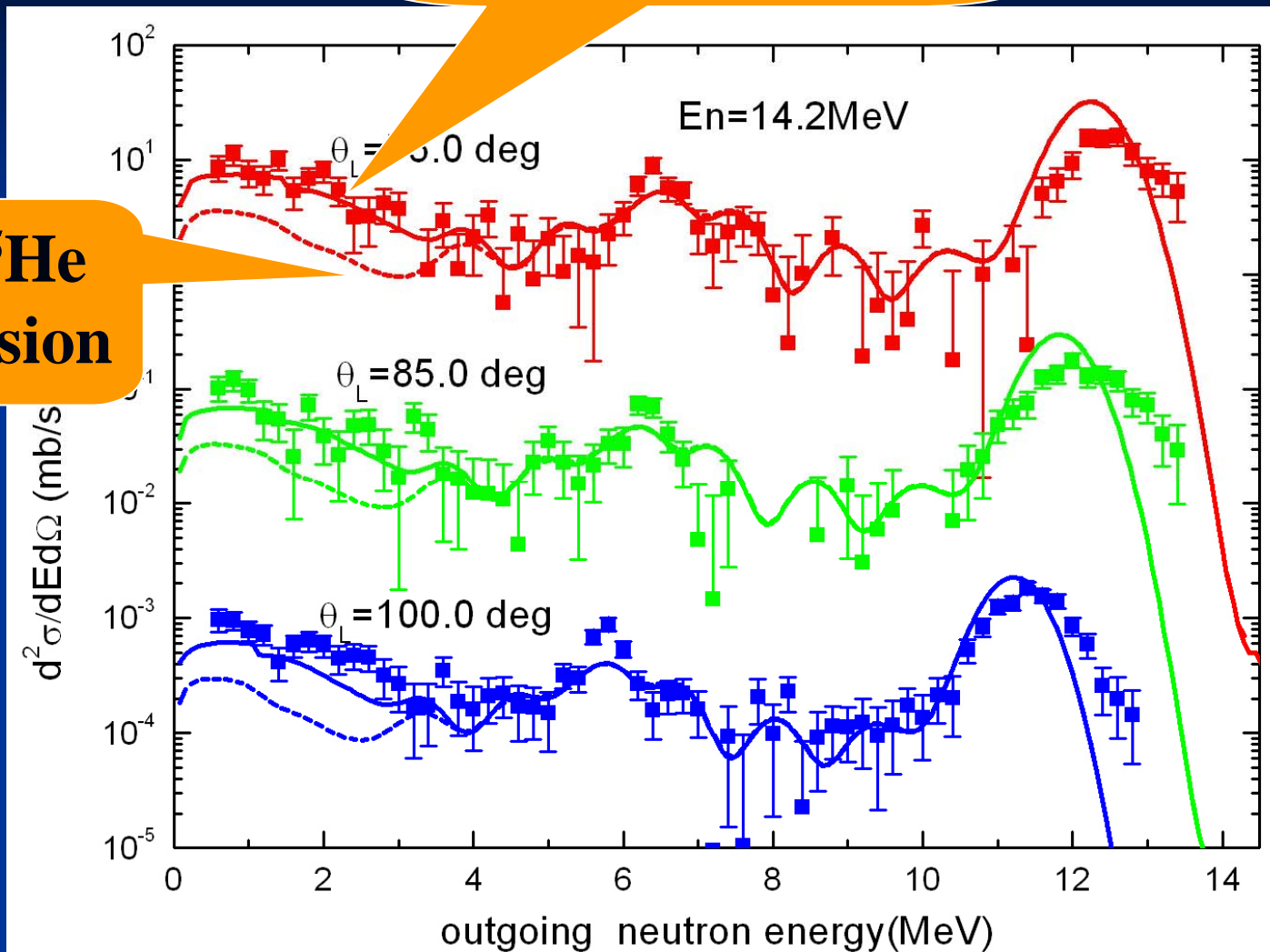
Open Channels (<20 MeV)

➤ **n + ¹⁰B**

$n + {}^{10}\text{B} =$	0	$\gamma + {}^{11}\text{B}$	$E_{th} = 0.0000$	$Q = 11.453$
	1	$n' + {}^{10}\text{B}$	$E_{th} = 7.9077$	$Q = -7.1840$
	2	$p + {}^{10}\text{Be}$	$E_{th} = 0.0000$	$Q = 0.225$
	3	$\alpha + {}^7\text{Li}$	$E_{th} = 0.0000$	$Q = 2.790$
	4	${}^5\text{He} + {}^6\text{Li}$	$E_{th} = 5.8944$	$Q = -5.3550$
	5	$d + {}^9\text{Be}$	$E_{th} = 4.8014$	$Q = -4.362$
	6	$t + {}^8\text{Be}$	$E_{th} = 0.0000$	$Q = 0.230$
	7	$2n + {}^9\text{B}$	$E_{th} = 9.2858$	$Q = -8.436$
	8	$(np + pn) + {}^9\text{Be}$	$E_{th} = 7.2494$	$Q = -6.586$
	9	$(n\alpha + \alpha n) + {}^6\text{Li}$	$E_{th} = 4.9082$	$Q = -4.459$
	10	$(nd + dn) + {}^8\text{Be}$	$E_{th} = 6.6341$	$Q = -6.027$
	11	$(p\alpha + \alpha p) + {}^6\text{He}$	$E_{th} = 7.9077$	$Q = -7.184$
12	$2\alpha + t$	$E_{th} = 0.0000$	$Q = 0.323$	

With ^5He emission

No ^5He emission



Nuclear model calculations

- (1) Study of Nucleus–nucleus microscopic optical potential and applications
- (2) Study of Folding model and application



Optical potential without free parameter
Application to unstable nuclei

(1) Study of Nucleus–nucleus microscopic optical potential and applications

Ma Yin-Qun and Ma Zhong-Yu

China Institute of Atomic Energy

Outline

1. The isospin dependent MOP of the nucleon-nucleus scatterings have been obtained in the framework of the DBHF approach, where the local density approximation is used.

$$V_{eff}^i = U_0^i + \frac{M}{E} U_s^i + \frac{1}{2E} [U_s^{i2} - (U_0^i - V_c)^2]$$

2. Extending this MOP to the case for a composite projectile based on folding model

$$V_{FM}(\vec{R}) = \frac{1}{(2\pi)^3} \sum_{i=p,n} \int \rho_i(\vec{k}_i) V_{eff}^i(\vec{k}_i) d\vec{k}_i$$

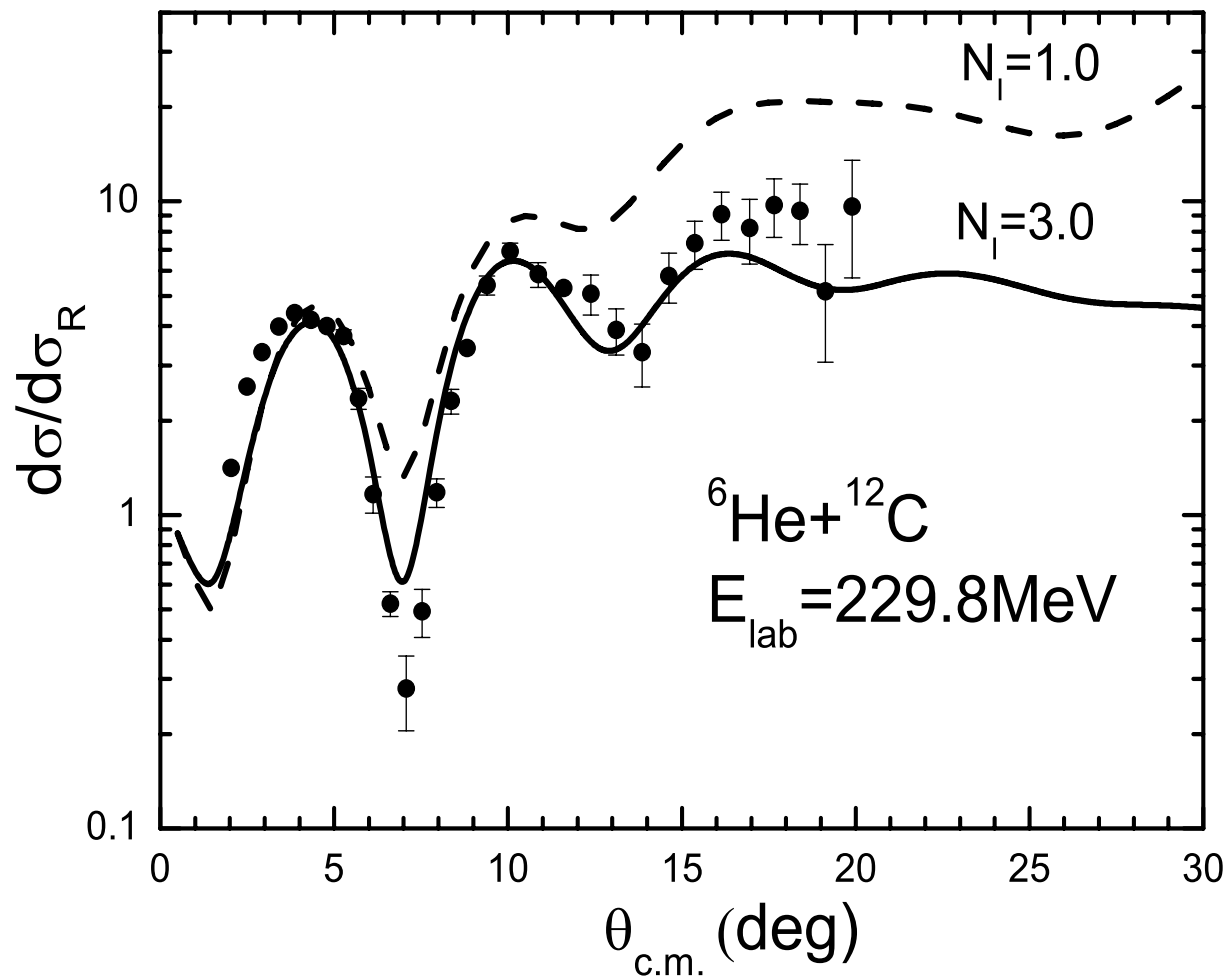
In the framework of momentum representivity

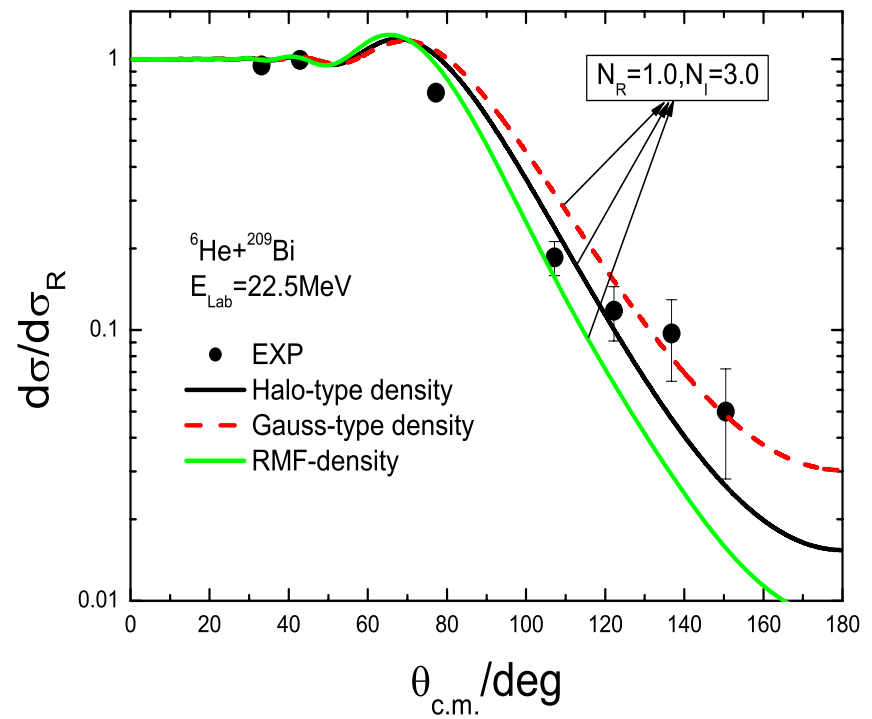
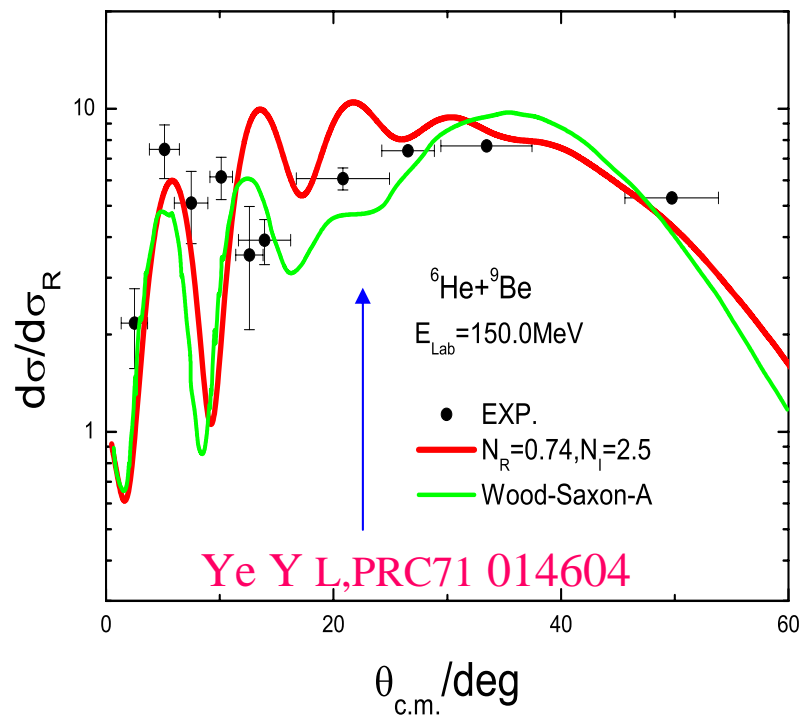
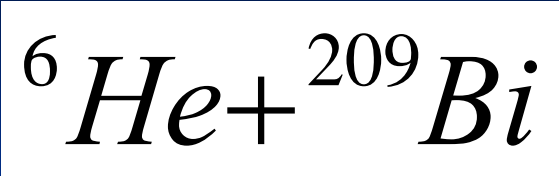
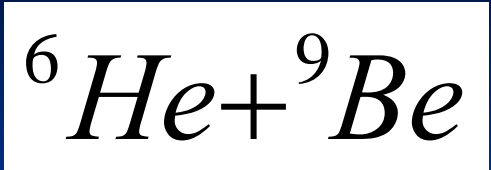
$$\begin{aligned} V_{FM}(R) &= V_{FM}^p(R) + V_{FM}^n(R) \\ &= \sum_{m=p,n} 4\pi \sum_l w_l^2 V_{eff}^m(k_l^2) \rho_m(k_l) j_0(k_l R) \\ &= \text{Re}V_{FM}(\mathbf{R}) + i\text{Im}V_{FM}(\mathbf{R}), \end{aligned}$$

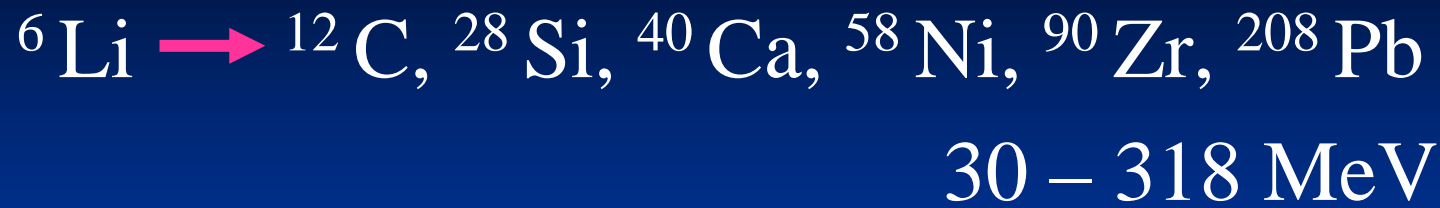
- In order to compare with experimental data, two normalization factors are introduced. Then, the optical potential is written as:

$$U_{opt}(\vec{R}) = N_R \text{Re}V_{FM}(\vec{R}) + N_I \text{Im}V_{FM}(\vec{R}) + U_C(\vec{R})$$

${}^6\text{He} + {}^{12}\text{C}$, elastic scattering

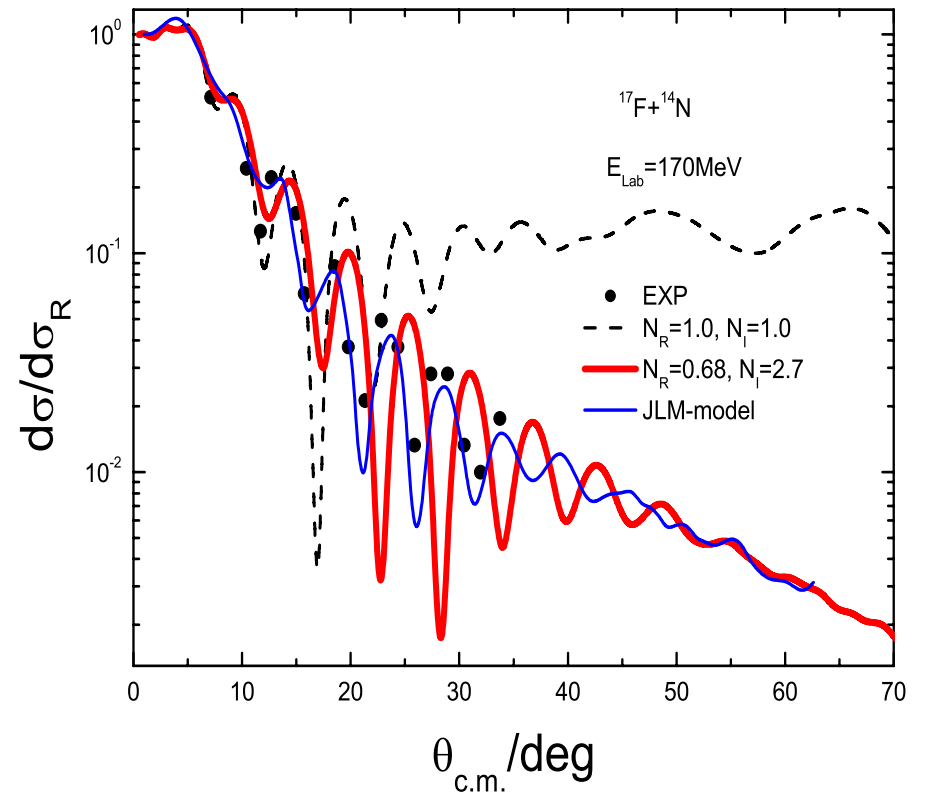
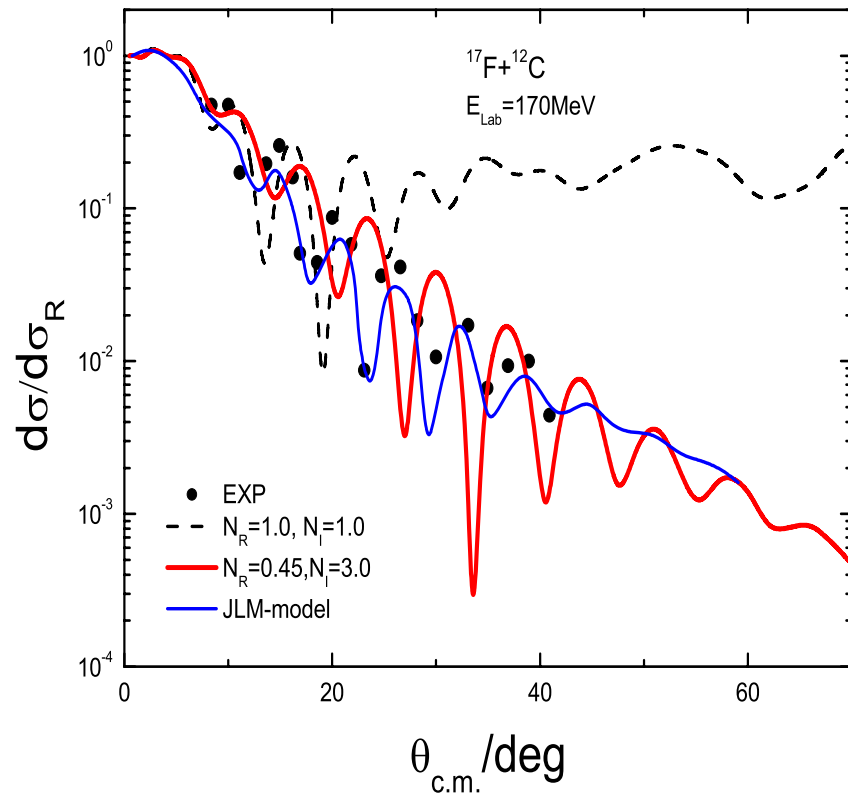
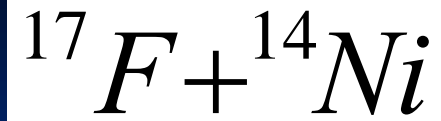
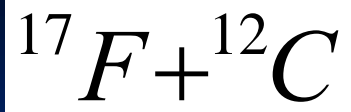


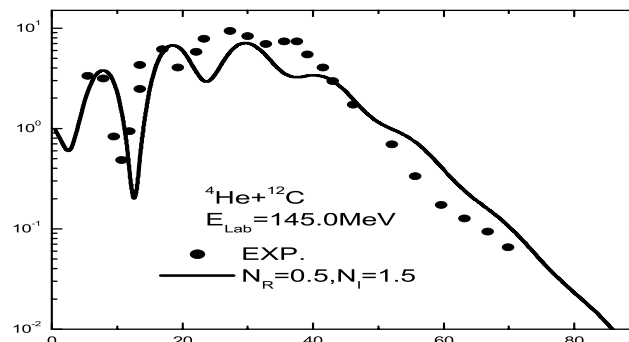
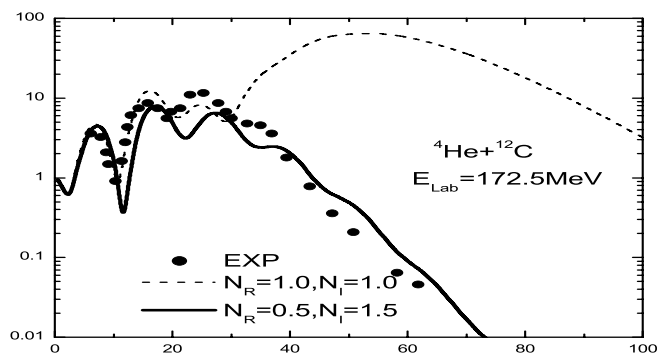




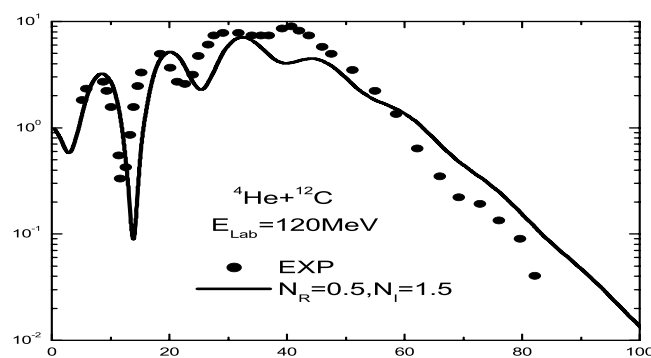
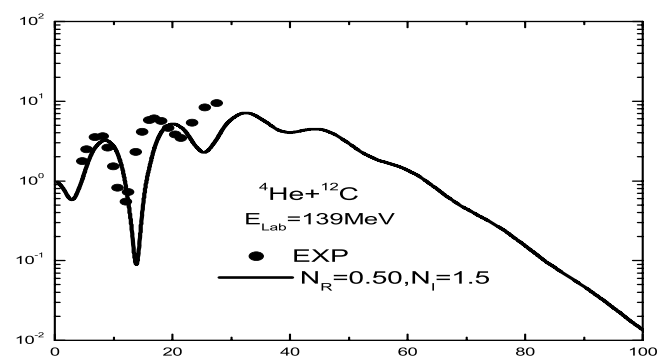
■ **neutron-rich nuclei**



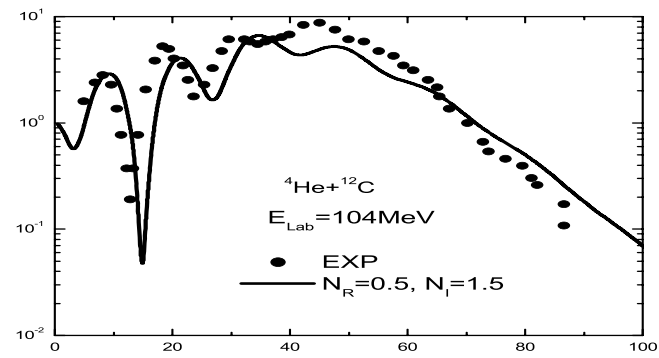




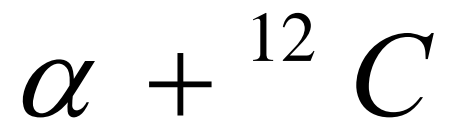
$d\sigma/d\sigma_R$

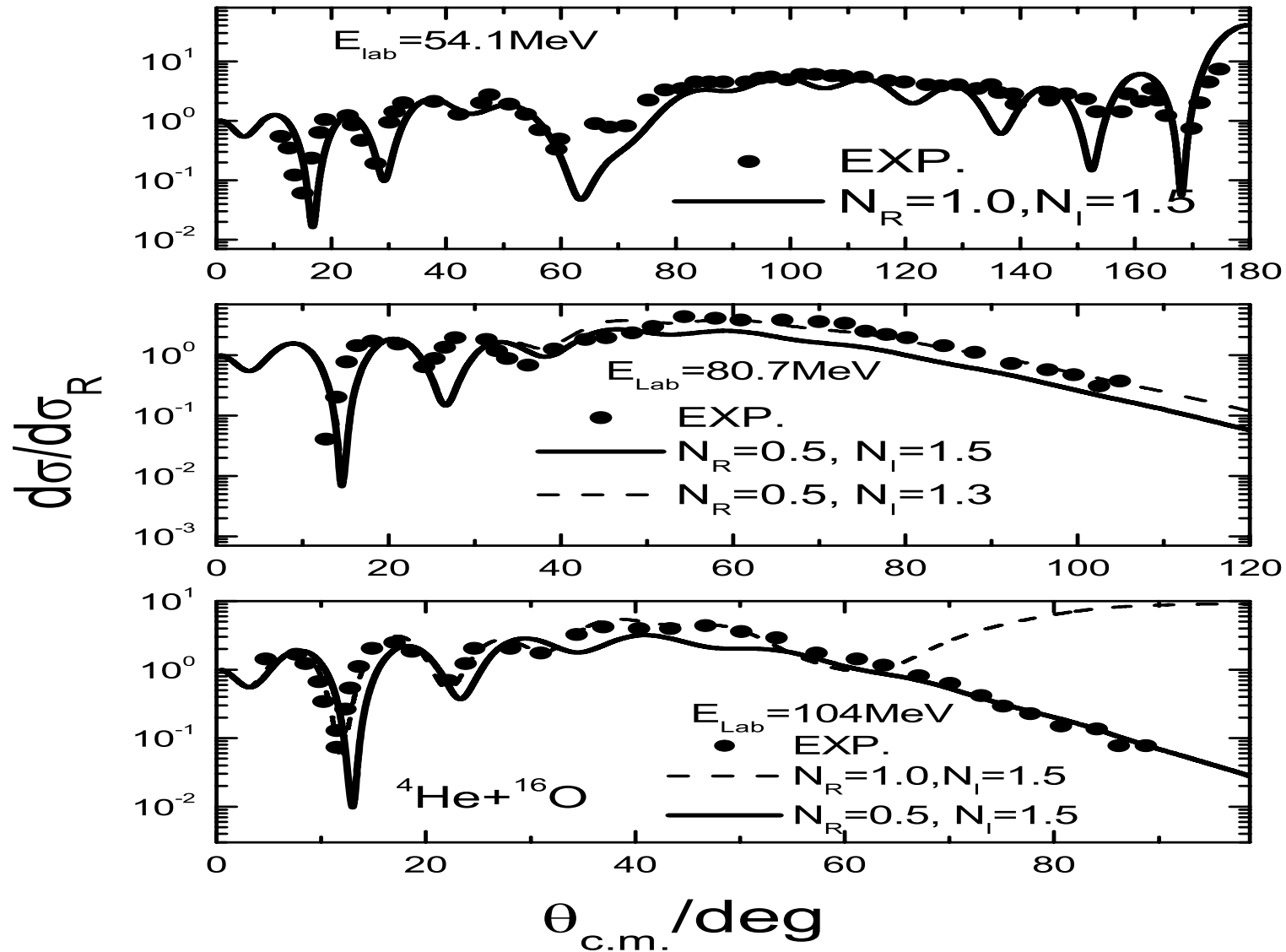
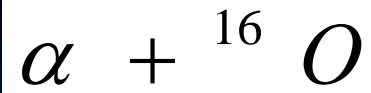


$\theta_{\text{c.m.}}/\text{deg}$



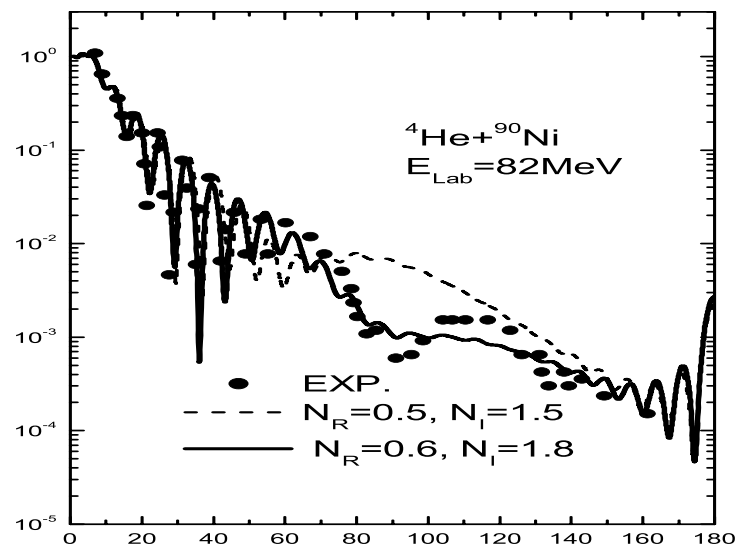
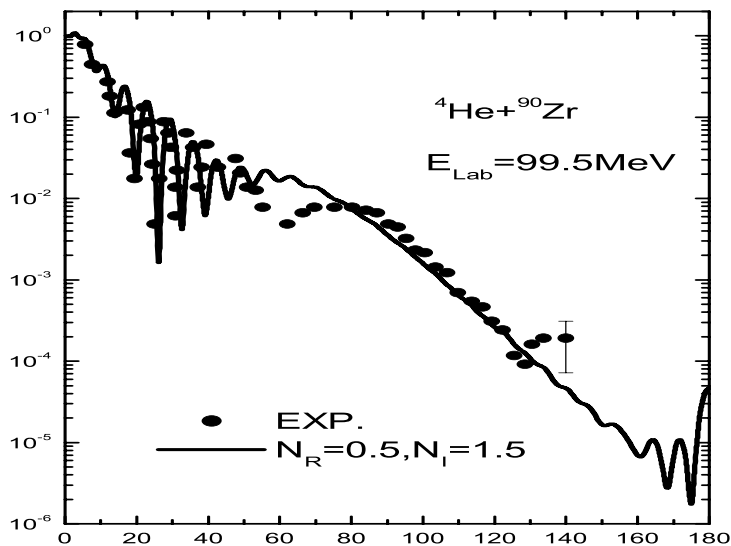
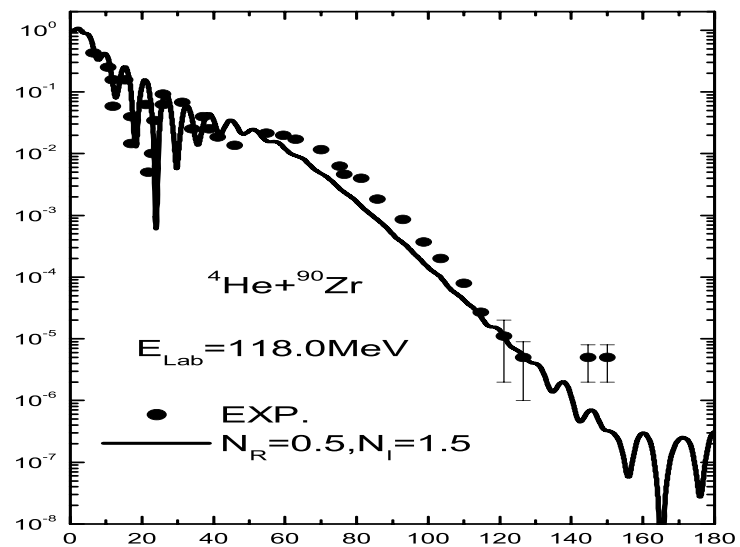
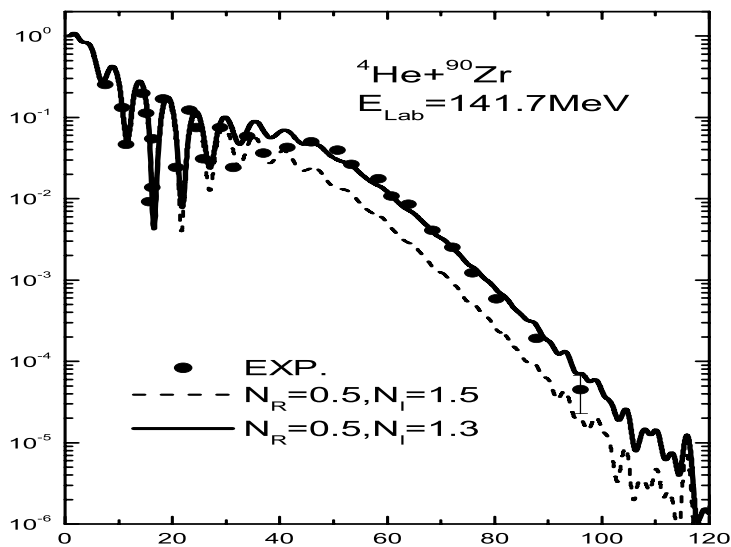
$\theta_{\text{c.m.}}/\text{deg}$





$\alpha + {}^{90}\text{Zr}$

$d\sigma/d\sigma_R$



$\theta_{c.m.}/\text{deg}$

(2) Study of Folding Model and Application

Nucleon-Nucleus interaction

$$V(E, r) = V_d(E, r) + V_{ex}(E, r)$$



Direct term



Exchange term

Khoa: Phys. Rev. C 63, 034007 (2001)

Isospin dependent interaction

CDM3Y

$$V(E, r) = \int d\mathbf{r}' \left\{ \left[\rho_p(\mathbf{r}') + \rho_n(\mathbf{r}') \right] v_{00}^d(\rho, E, s) \pm \left[\rho_p(\mathbf{r}') - \rho_n(\mathbf{r}') \right] v_{01}^d(\rho, E, s) \right\} \\ + \int d\mathbf{r}' \left\{ \left[\rho_p(\mathbf{r}, \mathbf{r}') + \rho_n(\mathbf{r}, \mathbf{r}') \right] v_{00}^{ex}(\rho, E, s) \right. \\ \left. \pm \left[\rho_p(\mathbf{r}, \mathbf{r}') - \rho_n(\mathbf{r}, \mathbf{r}') \right] v_{01}^{ex}(\rho, E, s) \right\} \exp(i\mathbf{k}(E, r)s)$$

One-body
Density matrix

One-body density Matrix

Campi and Bouyssy: “Local approximation”

$$\rho(\mathbf{R}, \mathbf{R} + \mathbf{s}) \approx \rho(\mathbf{R} + \mathbf{s}/2) \hat{j}_1 \left[k_F (\mathbf{R} + \mathbf{s}/2) s \right]$$

$$\hat{j}_1(x) = 3(\sin x - x \cos x) / x^3$$

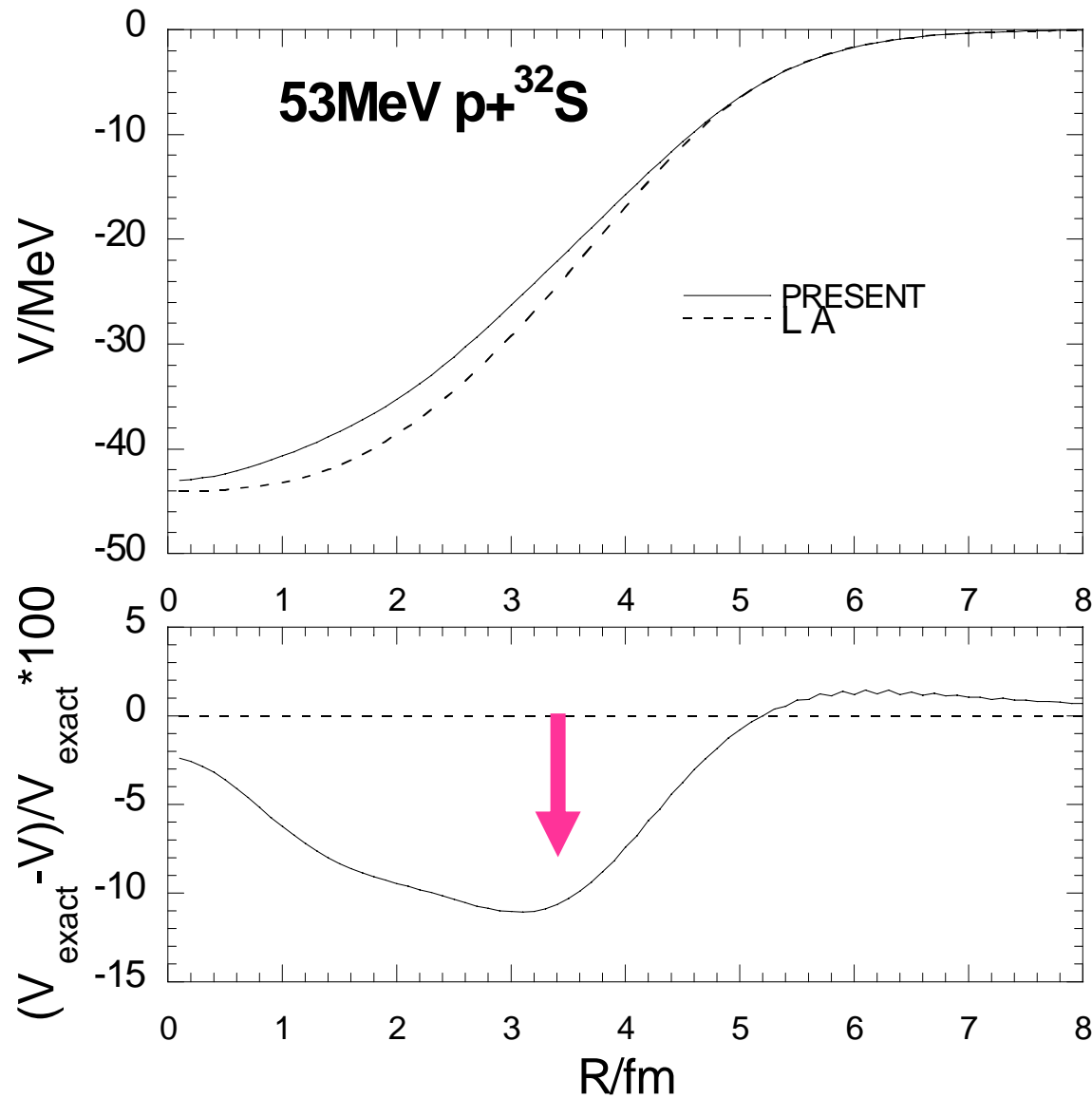
Calculation of one – body density matrix based on shell model

$$\rho(\mathbf{r}, \mathbf{r}') = \sum_{i=1}^A \sum_{\sigma} \varphi_i^*(\mathbf{r}, \sigma) \varphi_i(\mathbf{r}', \sigma)$$



Woods-Saxon potential

Comparison of folding potential by different one-body density matrix



10%

Optical potential

Normalization factor

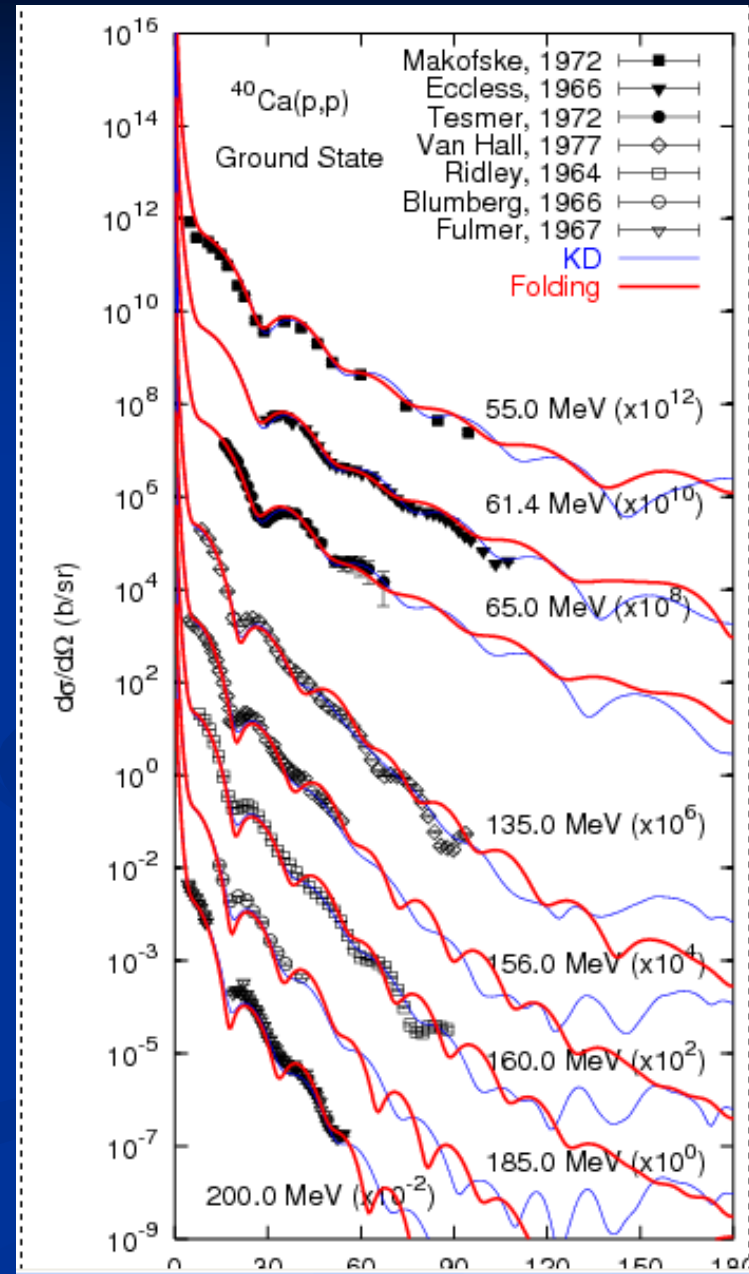
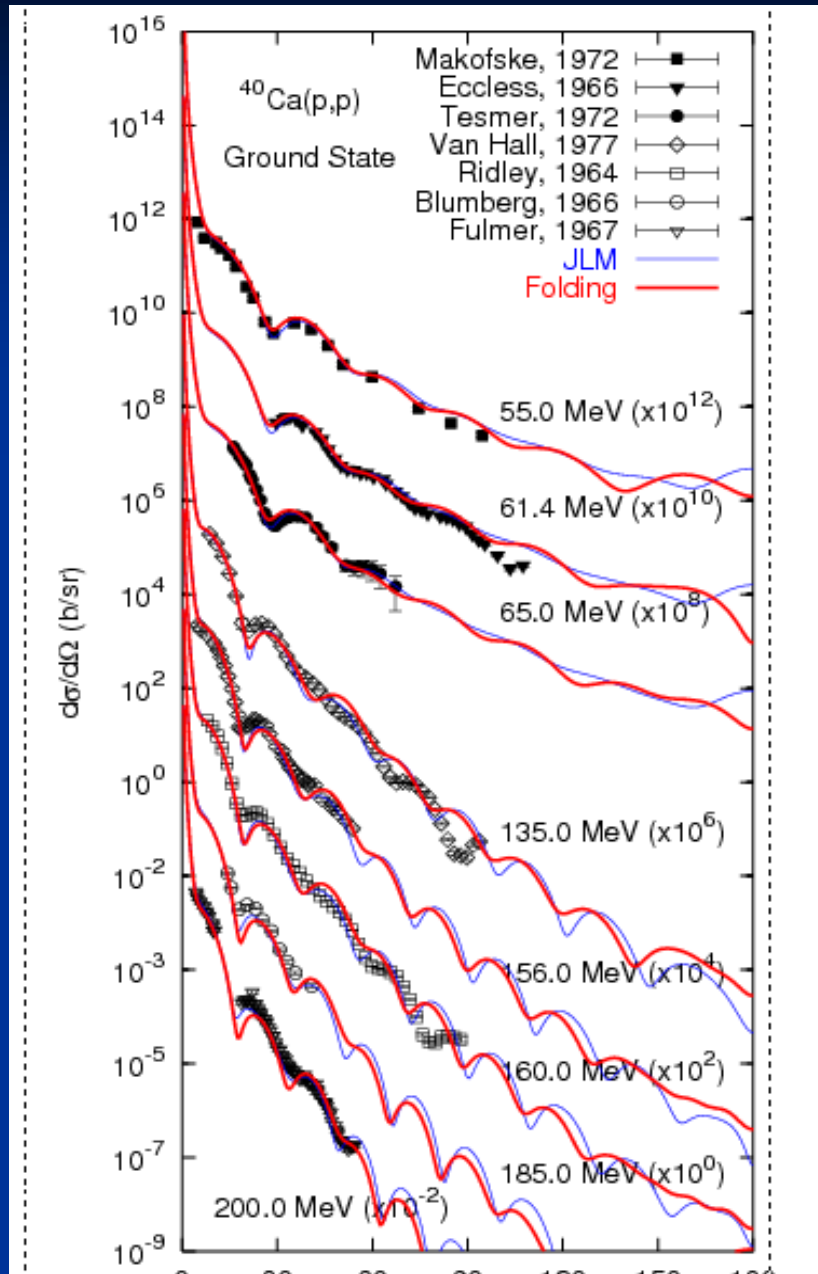
$$U(E, r) = Nr[V(E, r)] + iW(E, r) + V_{so}(E, r)(l \cdot \sigma) + V_C$$

Folding model

Phenomenal
Koning-Delaroche
potential

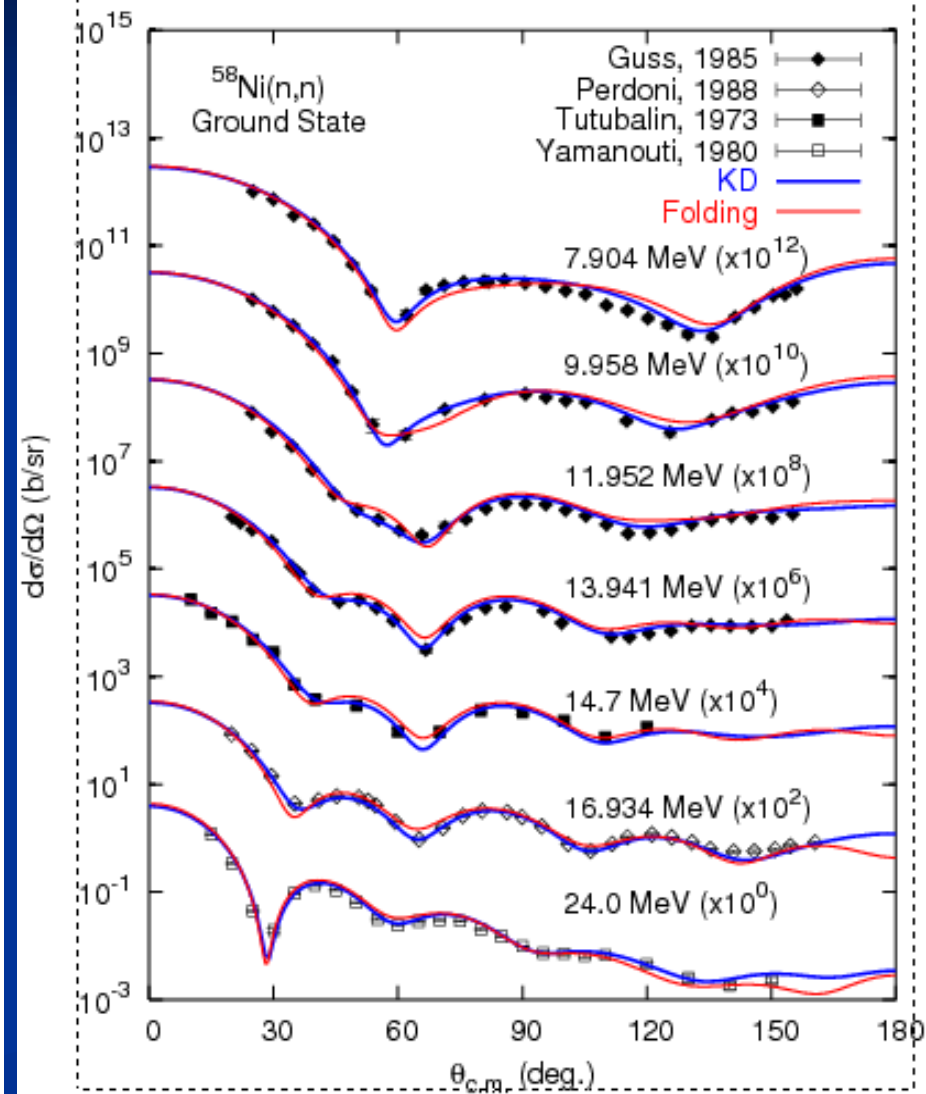
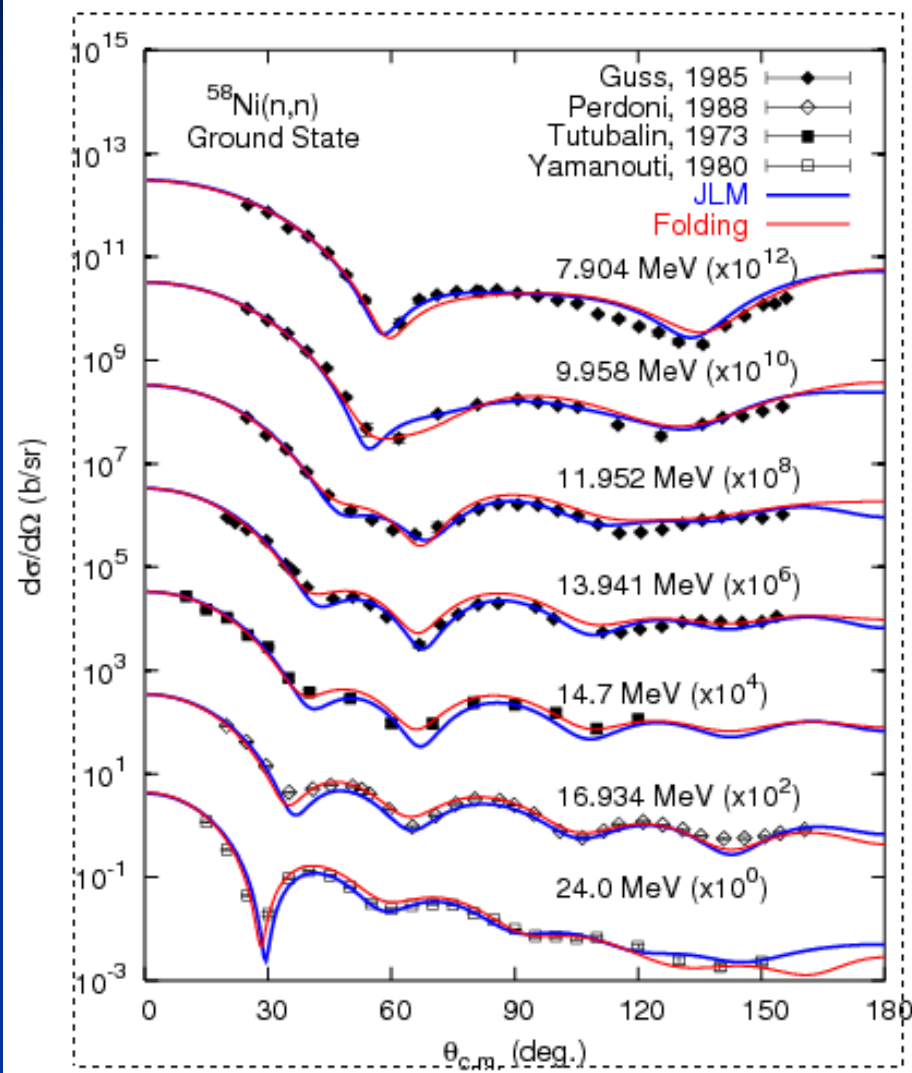
Folding vs JLM Folding vs KD

^{40}Ca
(p, p)



Folding vs JLM

Folding vs KD

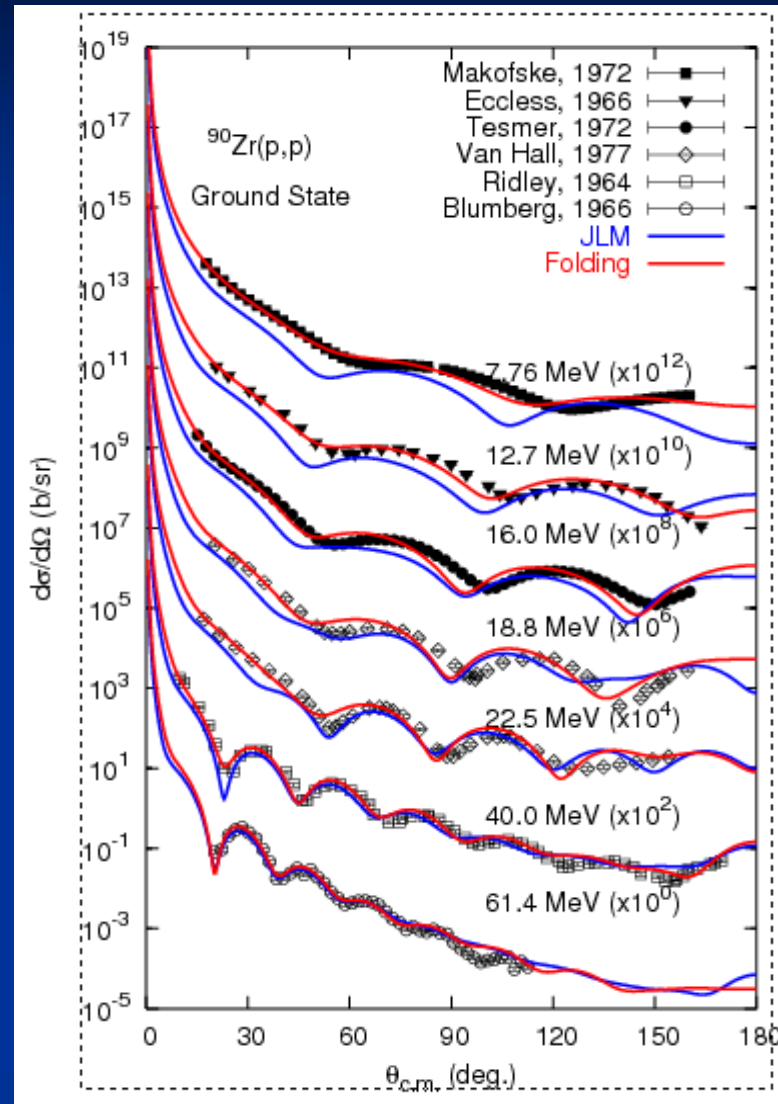


$^{58}\text{Ni}(n,n)$

$^{90}\text{Zr} (p, p)$

Folding vs JLM

7.76 -- 61.4 MeV

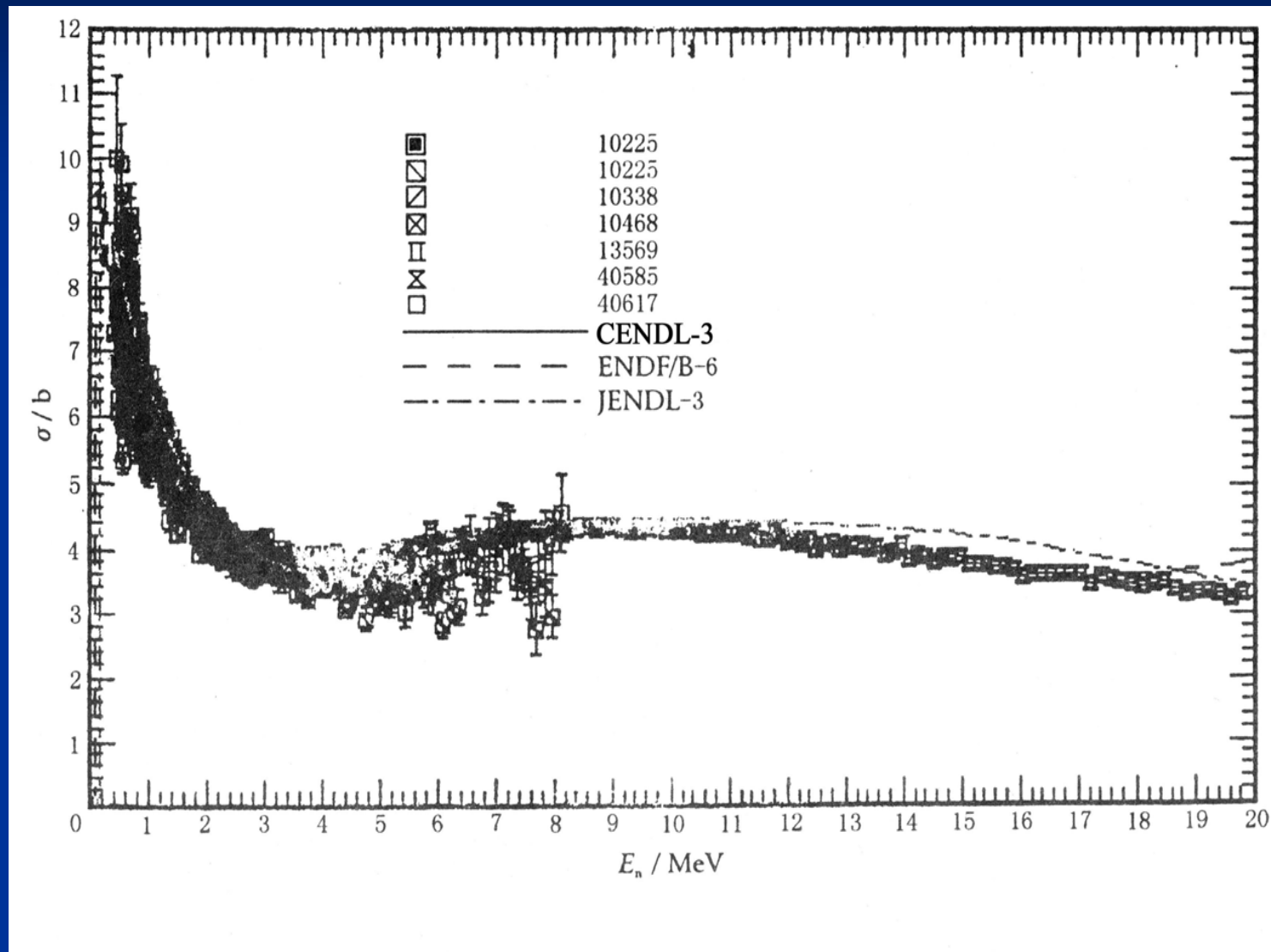


Thank you !!!

Structural materials (33)

Comparing to CENDL-2, the main development of CENDL-3.0 for the structured materials is that in addition to the data of natural elements, the data of their isotopes were also included, and made the data consistent between the natural elements and their isotopes.

The evaluated total cross section of $n + {}^{90}\text{Zr}$



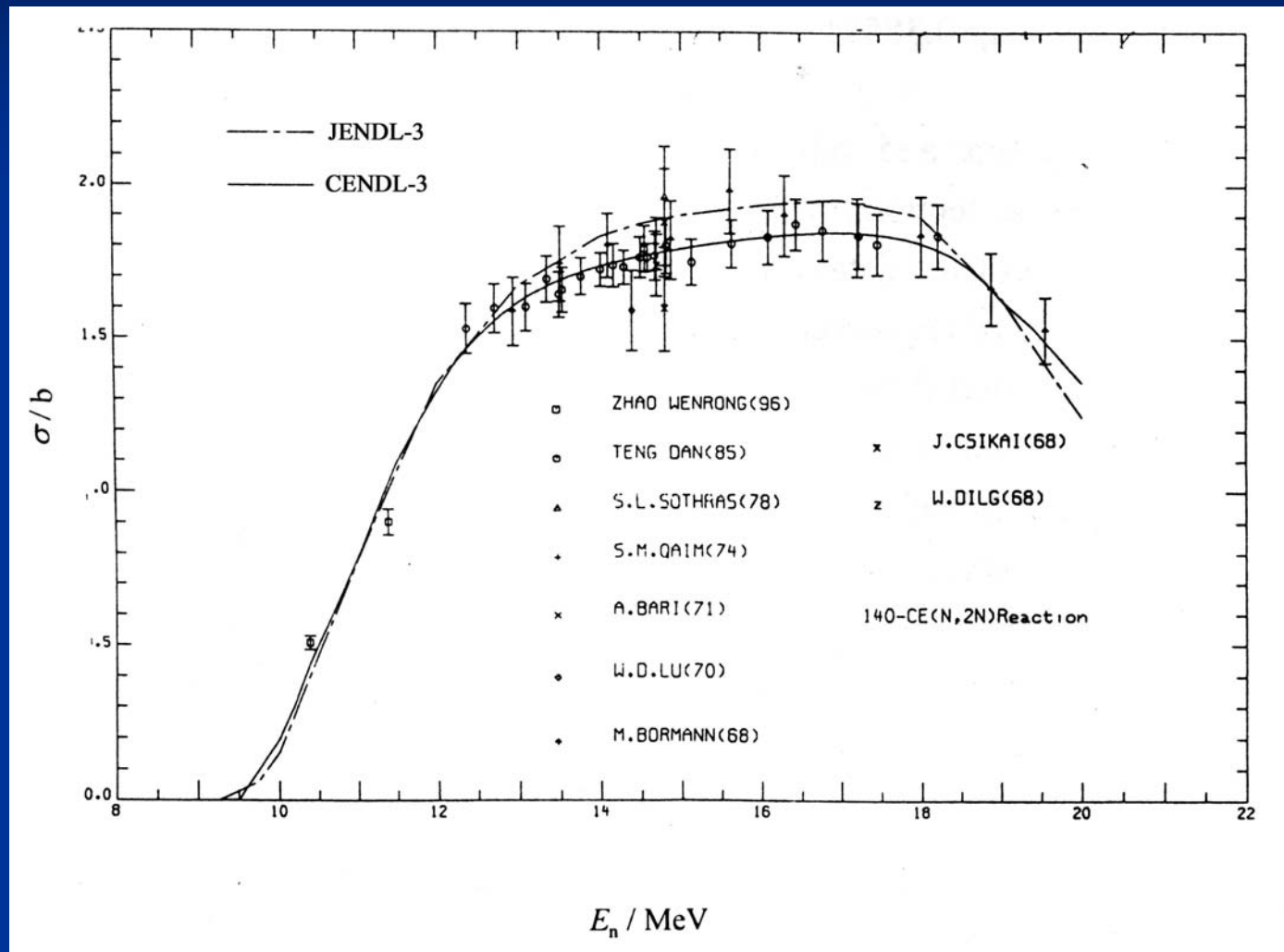
Fission products (115)

most fission products nuclides

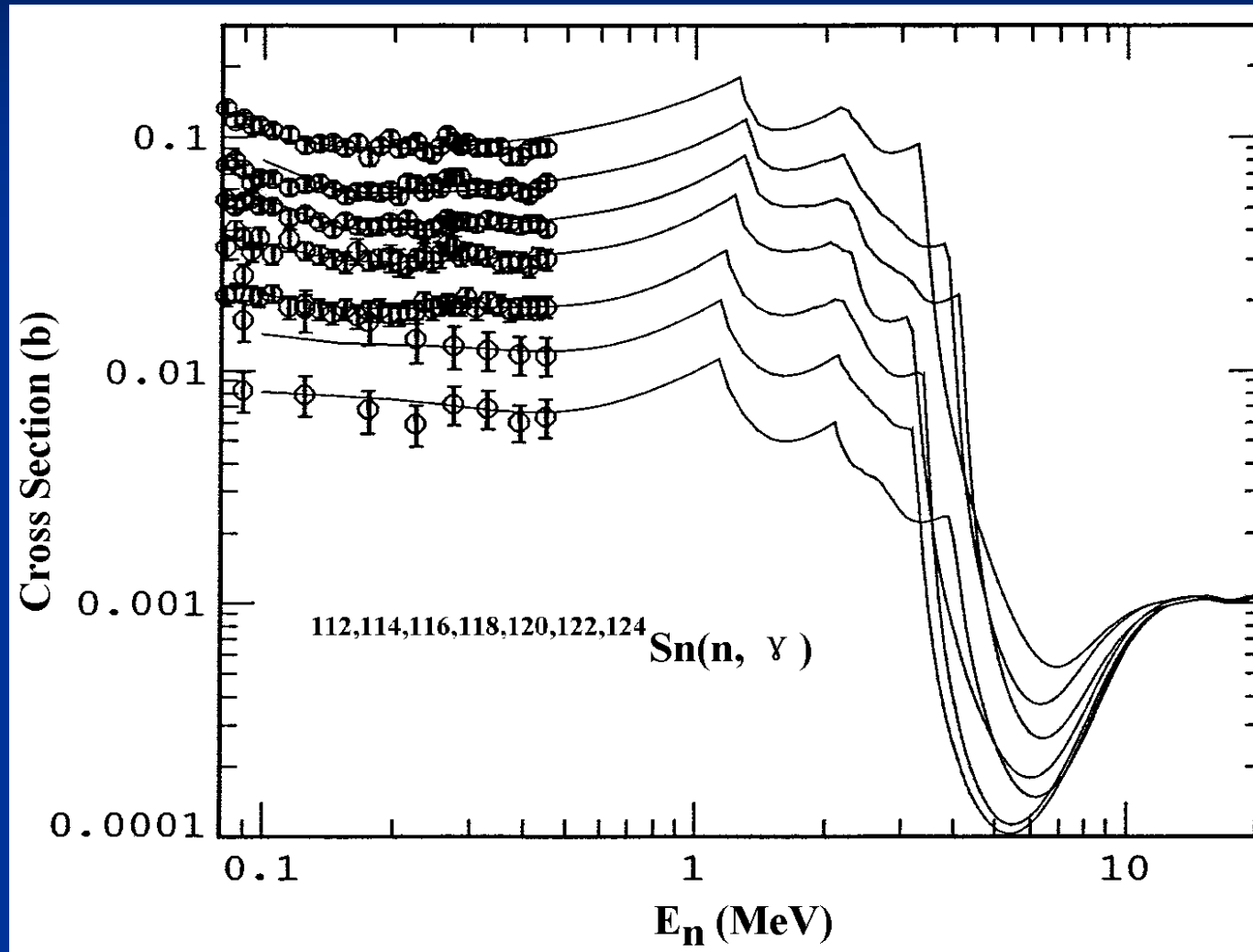
From MF-1 to MF-5 were provided in CENDL-3.0 for, MF-1 to MF-6 are variable for others.

101 fission products nuclides were sent to join in the international comparison of FP and coordinated by WPEC Subgroup 21, and 38 of them were selected as the data file of release 7 of ENDF/B-VI.

(n,2n) reaction cross section of n + ^{140}Ce



Sn (n, γ) capture cross section



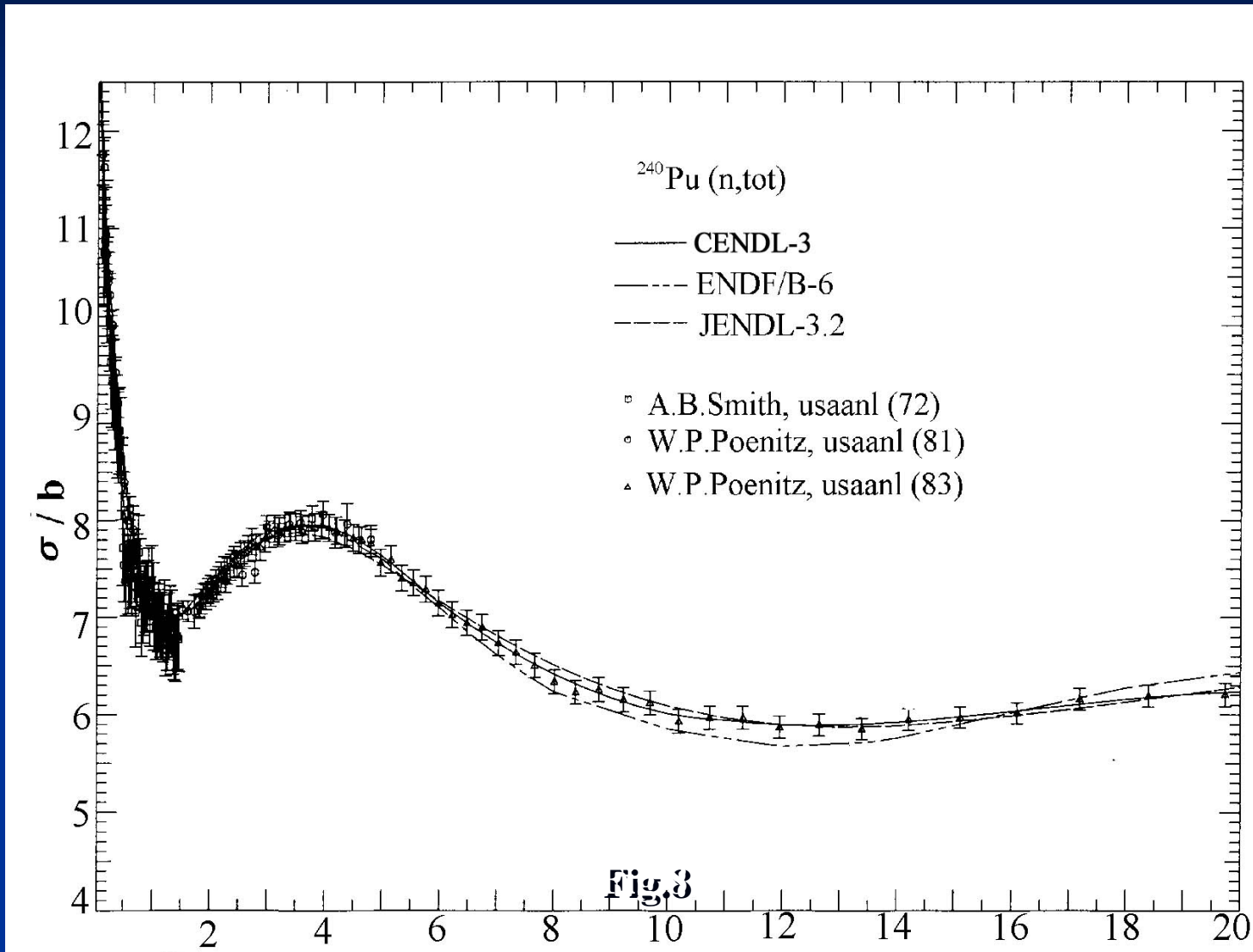
Actinides (18)

15 actinides were evaluated or re-evaluated.

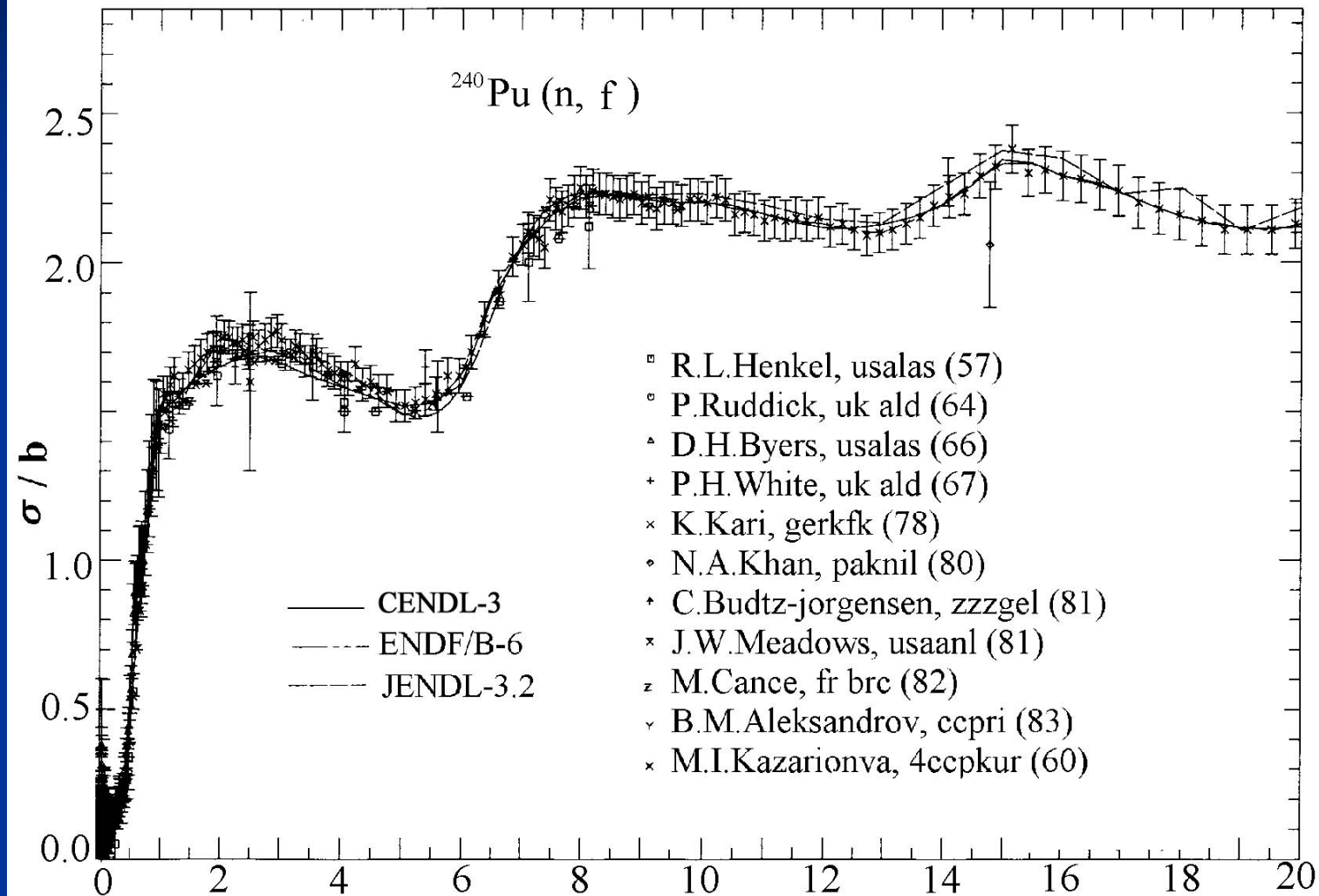
MF-1~6, 12~15 were included for important actinides (i.e. U, Pu isotopes), and MF-1~5 for others.

The results of the benchmark testing have been considered during the evaluation process.

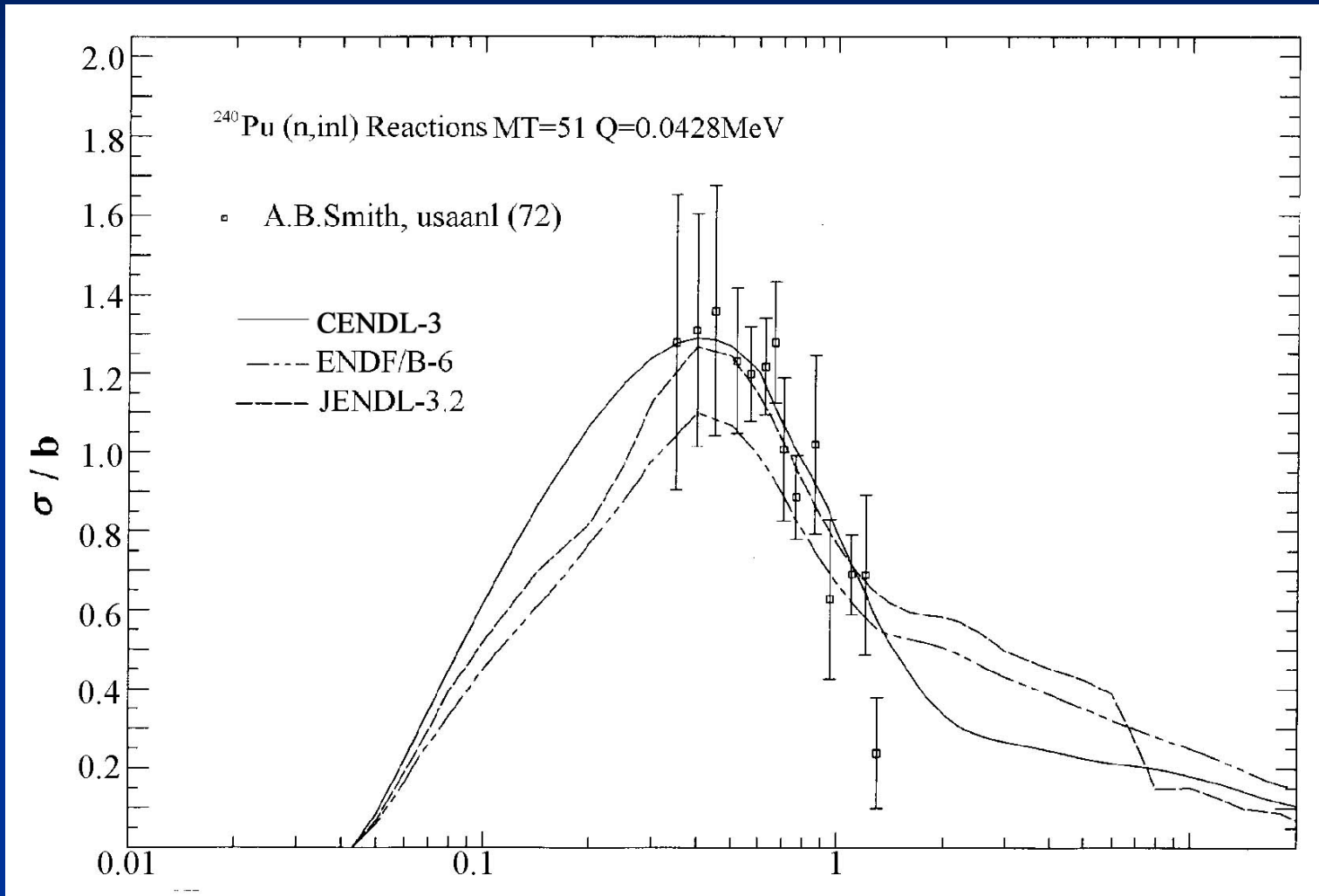
^{240}Pu (n, tot)



$^{240}\text{Pu} (n, f)$



^{240}Pu (n, inl) (MT=51)



1.3 The benchmark testing of CENDL-3.0

In order to test the reliability of the data from CENDL-3.0, benchmark testing for some important nuclides of CENDL-3.0 has been done, the calculations and analyses of benchmarks were done with Monte Carlo code MCNP and transformation codes. The data processing was carried out by using the internationally used code system NJOY97. The results were compared with ENDF, JENDL and JEFF validated CENDL-3.0 to identify the source of the discrepancies with the experimental results.

Table 1 and 2 show the results of calculation with different libraries K_{eff} of ^{233}U and ^{238}U as the examples.

Some of results based on benchmark FNS and OKTAVIAN for light and medium-heavy nuclides of CENDL-3.1 are presented here (Fig.11-13).

K_{eff} for ^{233}U

Assembly	Experiment	CENDL-3.0	ENDF/B-VI	JENDL-3.2
233U Jezebel	1.000(\sim 0.001)	0.99822	0.99235	1.01460
233U-F-002a	1.000(\sim 0.001)	0.99518	0.99544	1.00799
233U-F-002b	1.000(\sim 0.001)	0.99583	0.99943	1.00959
233U-F-003a	1.000(\sim 0.001)	0.99474	0.99755	1.01168
233U-F-003b	1.000(\sim 0.001)	0.99523	0.99989	1.00929
233U-F-004a	1.000(\sim 0.001)	1.00715	1.00494	1.01747
233U-F-004b	1.000(\sim 0.001)	1.00808	1.00940	1.01721
233U-F005a	1.000(\sim 0.001)	0.99951	0.99409	1.00852
233U-F-005b	1.000(\sim 0.001)	1.00204	0.99803	1.00763
Flattop-23	1.000(\sim 0.001)	0.99218	1.00146	1.01140
Averaging	1.000(\sim 0.001)	0.99882	0.99926	1.01154

Keff for ^{238}U

Benchmarks of Thermal Reactor

Assembly	CENDL-3.0	JEF-2	JENDL-3.2	ENDF/B-6
TRX-1	0.9975	0.9952	0.9901	0.9908
TRX-2	0.9998	0.9972	0.9920	0.9924
BAPL- UO_2 -1	1.0010	1.0020	0.9975	0.9952
BAPL- UO_2 -2	1.0003	1.0014	0.9972	0.9951
BAPL- UO_2 -3	1.0007	1.0014	0.9976	0.9960

Conclusion

1. CENDL-3.0 was finished in 2000, and it has been improved since then. CENDL-3.1 is be preparing for its release.
2. Nuclides and data files of CENDL-3.1 were increased and extended compared with CENDL-2.1.
3. All evaluations performed based on the new experimental data and model calculations carefully. They were improved compared with CENDL-2.1.
4. The data of the most important nuclides were validated by the benchmark testing. Some of them are better than other evaluated libraries according to the results of the benchmark testing .

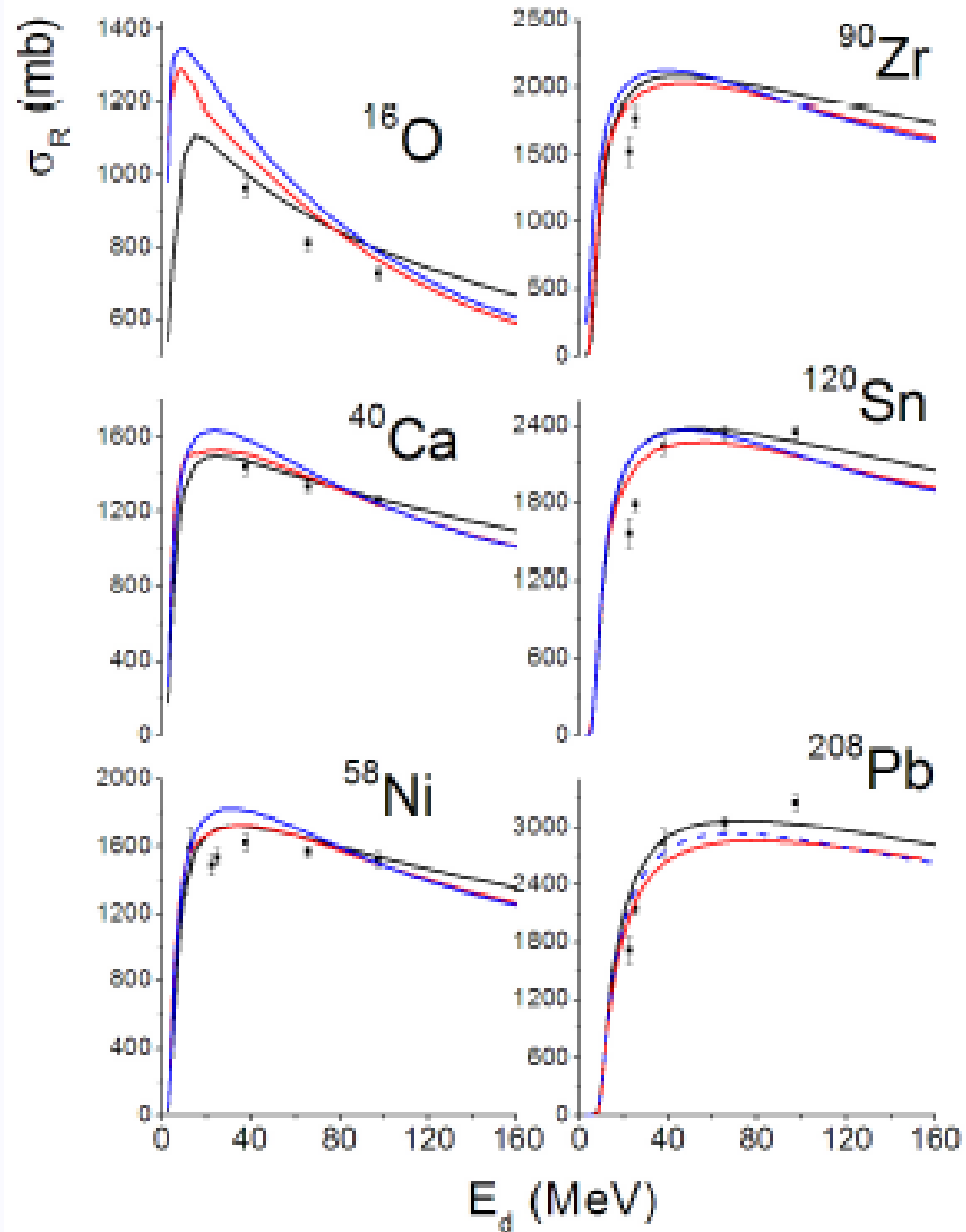
2.4 Nuclear structure and decay data

CNDC has taken permanent responsibility for evaluating and updating NSDD for A=51, and 195-198 mass chain. The data have been revised using available experimental decay and reaction data for mass chain A=197, and are being updated for mass chain A=196. Updated evaluation of A=197 has been sent to NNDC, USA and was published in NDS in 2004. The evaluations of mass chain A=52-56 were being updated at Jilin University. The decay data of ^{233}U were being evaluated on the basis of the new measured data.

2.3 The systematic study of fission yield data

Based on the mass distribution data up to 200 MeV measured by Zoller, the systematic on dependence of chain yield on incident neutron energy for each mass number A was studied. And also the systematics of mass distribution on mass A and incident neutron energy was investigated by using 5 (or 3) Gaussian model. The calculated results could reproduce the experimental data used well. The investigation also shows that the correlation between the parameters of the systematic and the yields calculated with the systematics is quite complicated and, in general, is quite strong.

Reaction Cross Section



CDM3Y nucleon-nucleon Interaction

$$v_{00(01)}^{\text{d(ex)}}(\rho, E, s) = F(\rho) g(E) v_{00(01)}^{\text{d(ex)}}(s)$$

$$v_{00(01)}^{\text{d(ex)}}(s) = \sum_{\nu=1}^3 Y_{00(01)}^{\text{d(ex)}} \frac{\exp(-R_{\nu} s)}{R_{\nu} s}$$

Isospin dependent interaction

$$\begin{aligned} V(E, r) = & \int d\mathbf{r}' \left\{ [\rho_p(\mathbf{r}') + \rho_n(\mathbf{r}')] v_{00}^d(\rho, E, s) \pm [\rho_p(\mathbf{r}') - \rho_n(\mathbf{r}')] v_{01}^d(\rho, E, s) \right\} \\ & + \int d\mathbf{r}' \left\{ [\rho_p(\mathbf{r}, \mathbf{r}') + \rho_n(\mathbf{r}, \mathbf{r}')] v_{00}^{ex}(\rho, E, s) \right. \\ & \left. \pm [\rho_p(\mathbf{r}, \mathbf{r}') - \rho_n(\mathbf{r}, \mathbf{r}')] v_{01}^{ex}(\rho, E, s) \right\} \exp(i\mathbf{k}(E, r) s) \end{aligned}$$

Code:

LUNF : **Light elements**

SUNF : **Structural Materials, fission products**
Medium elements

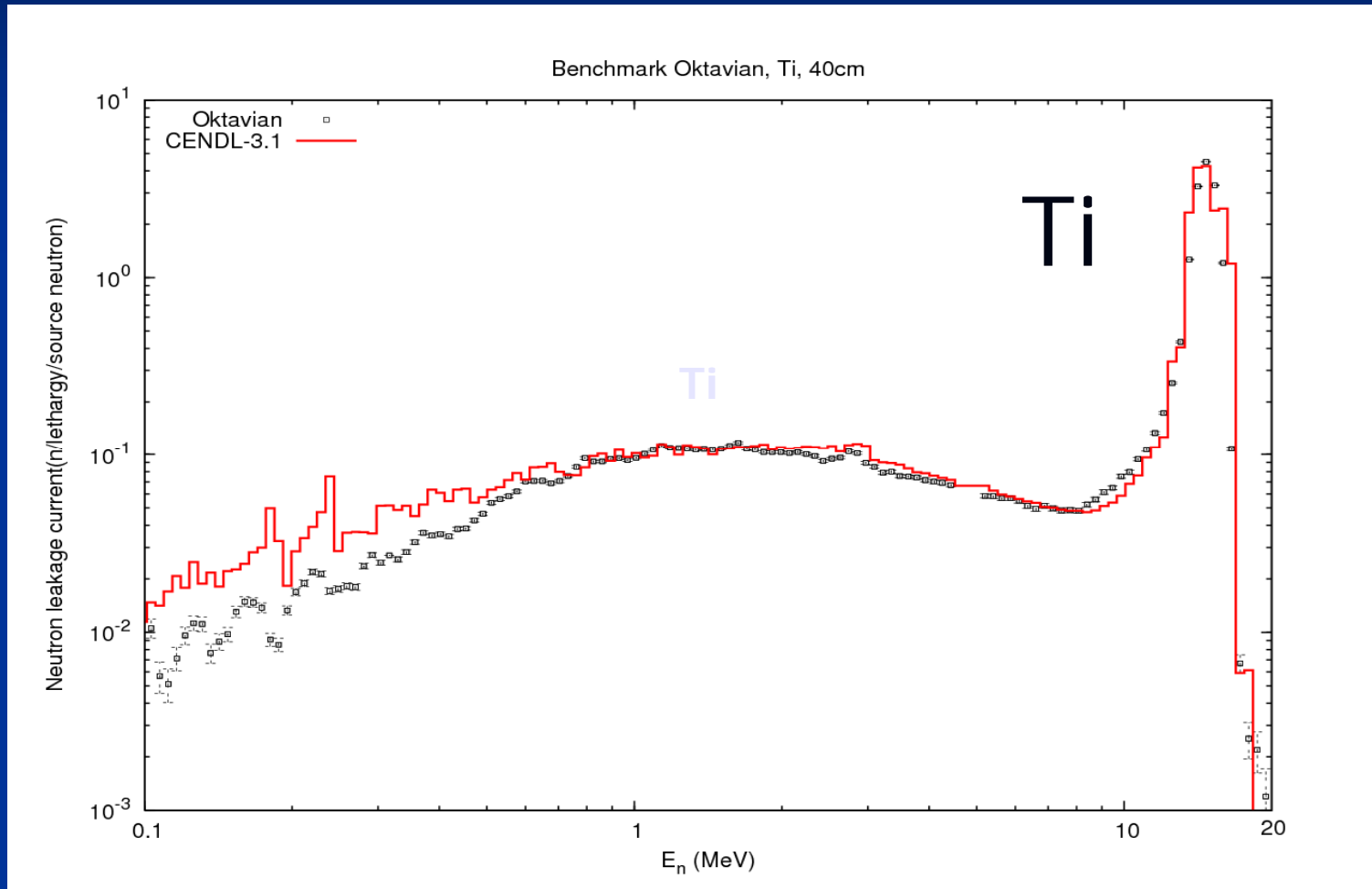
FUNF : **Heavy elements & actinides**

APMN/APOM94: **spherical optimal potential**

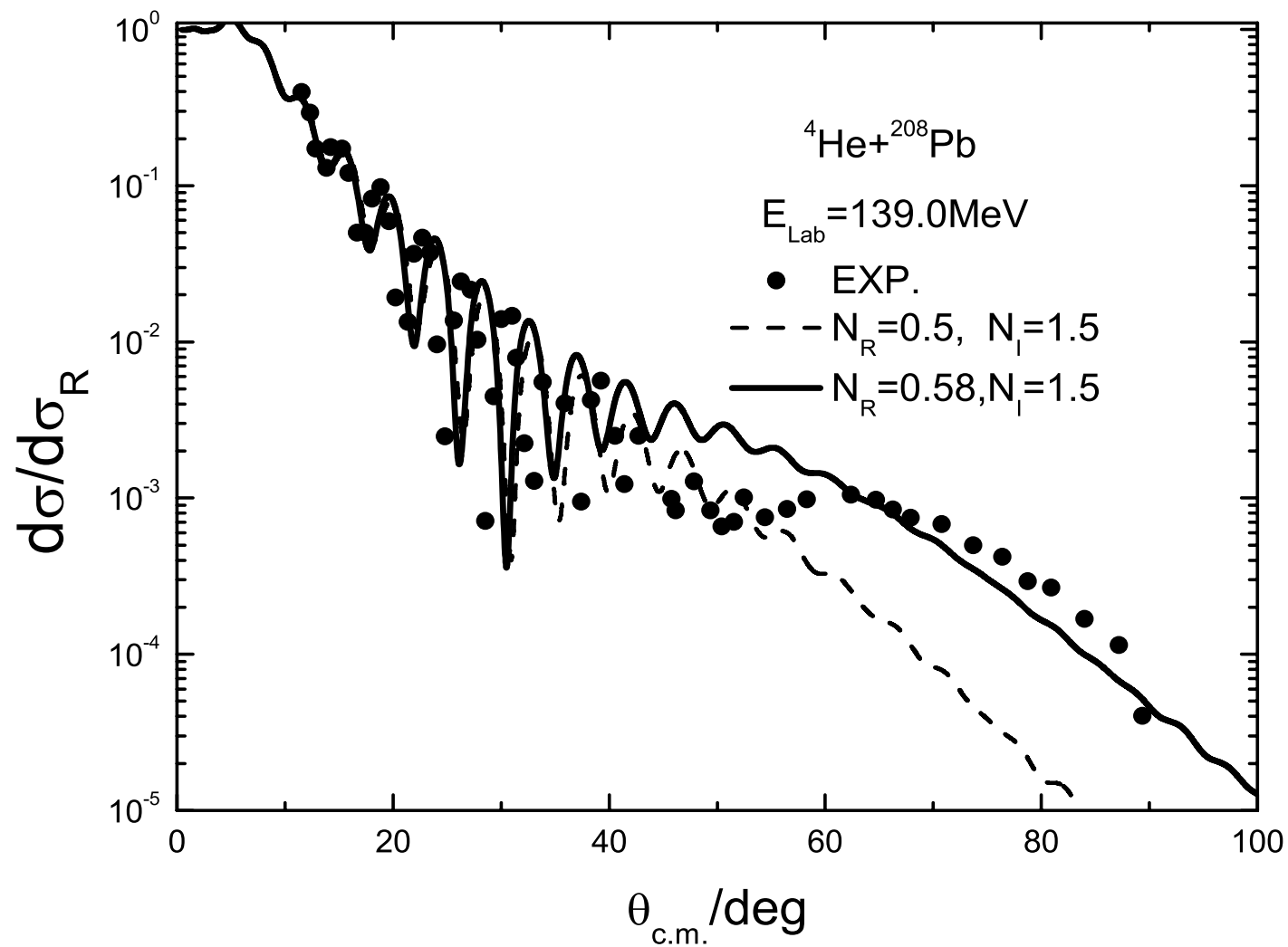
DWUCK + ECIS: **inelastic / deformed nuclei**

INPUT: RIPL + adjust

Neutron spectrum for the OKTAVIAN Ti



$\alpha + {}^{208}\text{Pb}$



Plan

2006 --- 2010

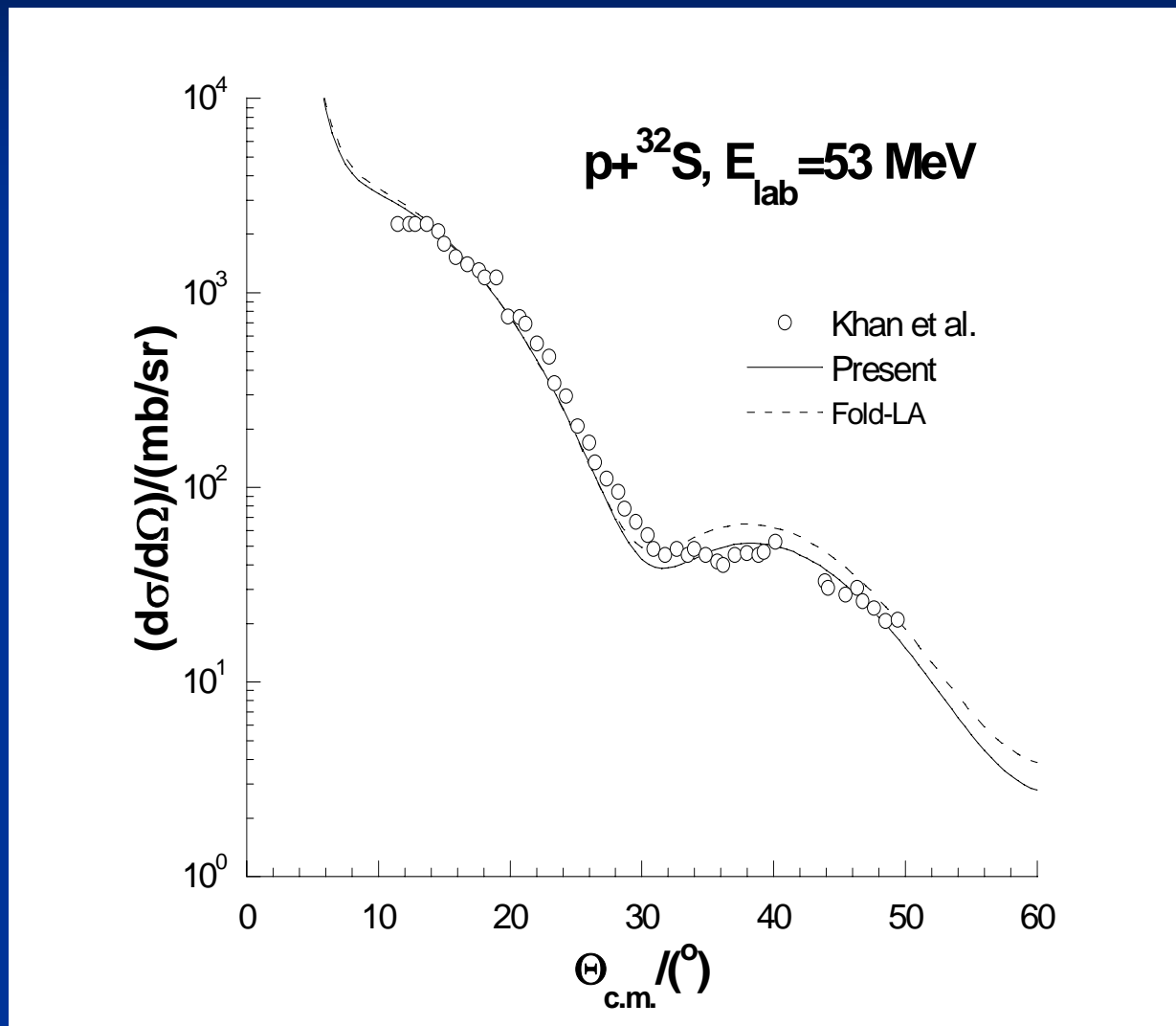
- More than 100 nuclides will be evaluated.
- Revision and validation.
- covariance data.

CDM3Y nucleon-nucleon Interaction

$$v_{00(01)}^{\text{d(ex)}}(\rho, E, s) = F(\rho) g(E) v_{00(01)}^{\text{d(ex)}}(s)$$

$$v_{00(01)}^{\text{d(ex)}}(s) = \sum_{\nu=1}^3 Y_{00(01)}^{\text{d(ex)}} \frac{\exp(-R_{\nu} s)}{R_{\nu} s}$$

Comparison of elastic angular distribution



II. Progresses on nuclear data evaluations

2.1 Nuclear reaction model study

The model was improved and completed for 1p shell light nuclides, which contains the dynamics and kinematics of nuclear reactions.

A method to set up file-6 of light nuclei for evaluated neutron data in ENDF/B-6 format below 20 MeV has been established and the energy balance was strictly considered. This method has been used in the calculation of $n + {}^{12}\text{C}$.

The possibility of ${}^5\text{He}$ emission has been investigated in the light nuclear reactions, and the formulation for calculating of the ${}^5\text{He}$ emission was developed. Also the double differential cross sections of ${}^5\text{He}$ emission, as well as the spectra of neutron and alpha particle from the breakup of ${}^5\text{He}$, were set up and used in the series codes of LUNF.

(2) Study of CDCC approach and application

An Haixia and Cai Chonghai

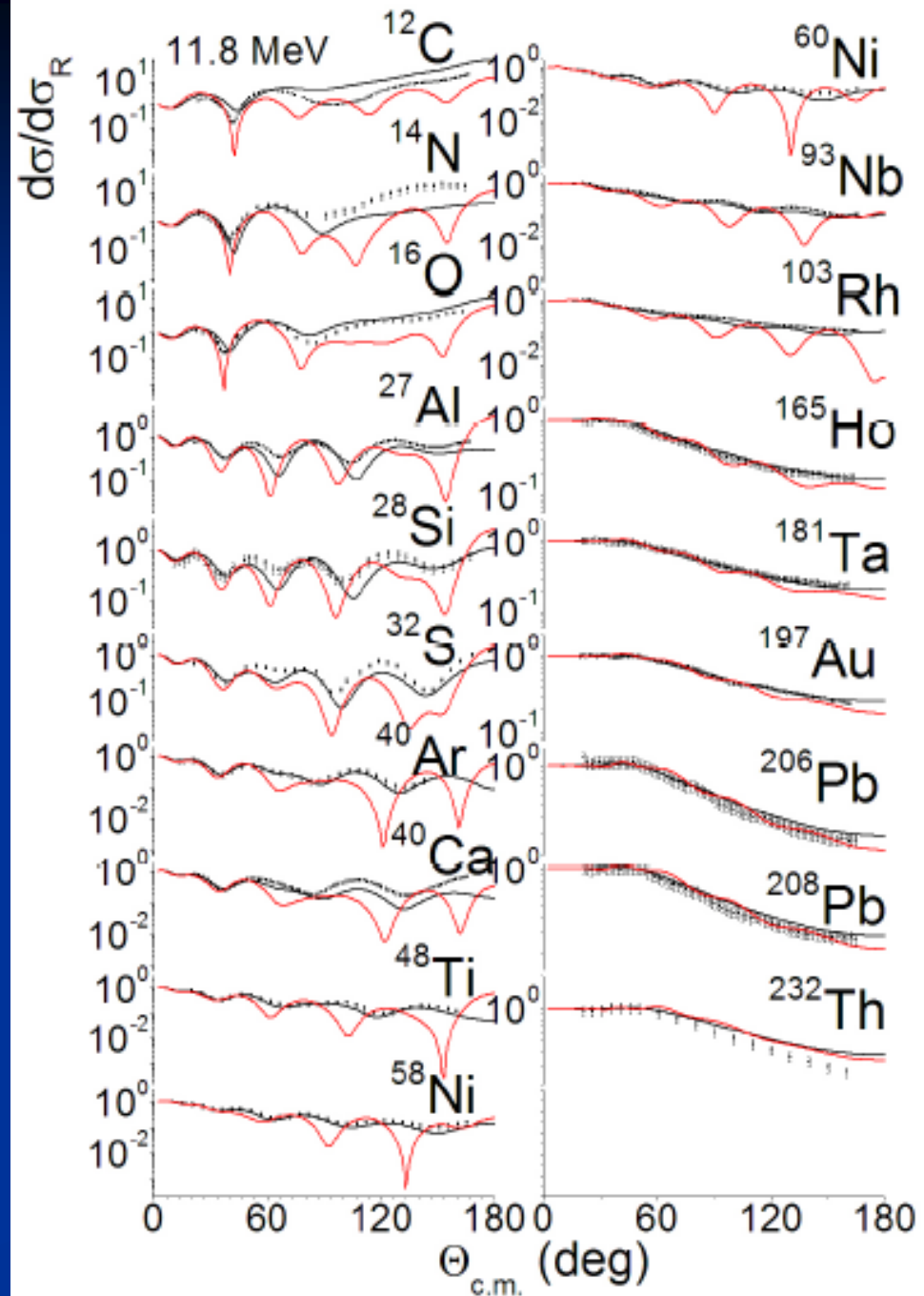
NanKai University

outline

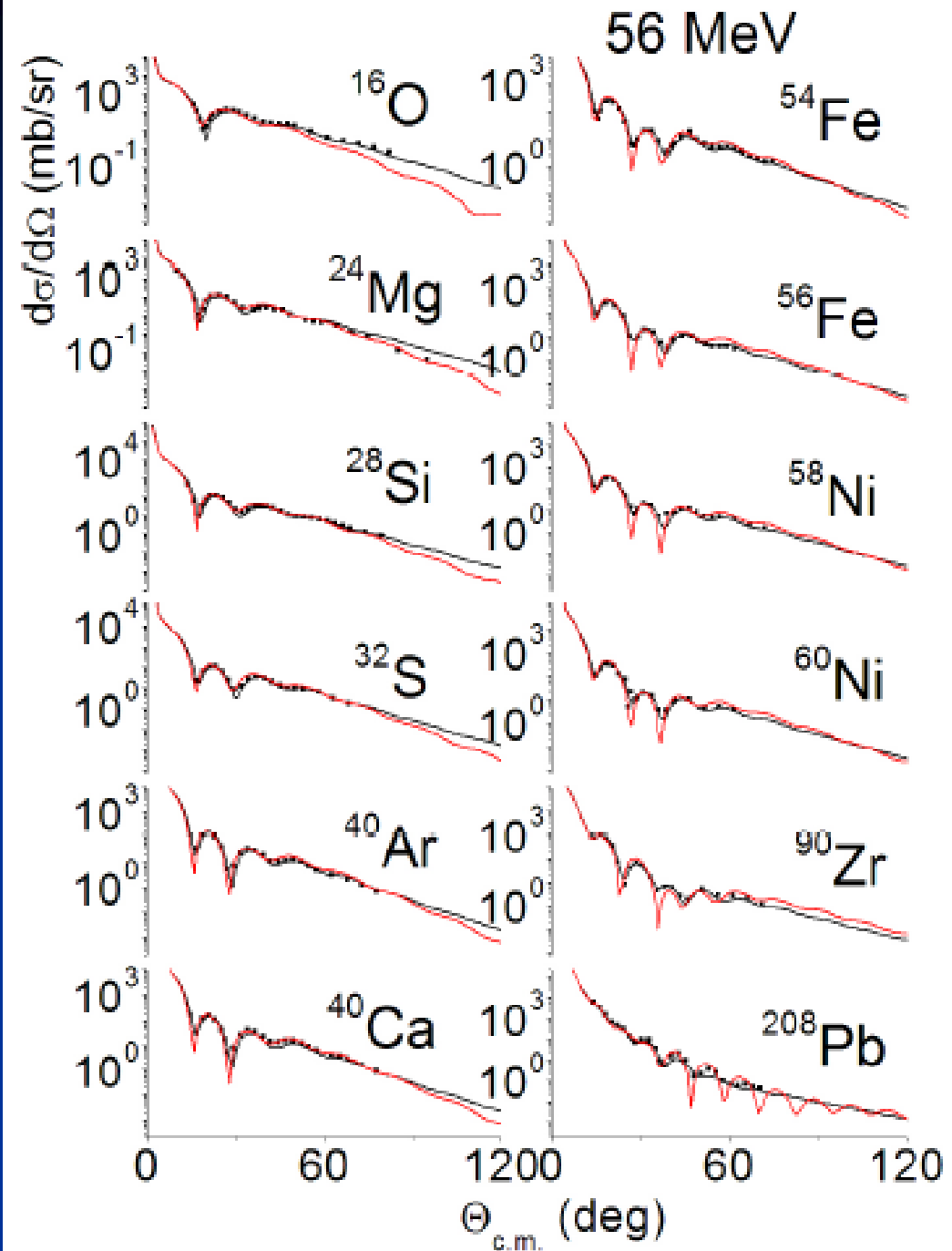
- A new code is developed based on CDCC approach and P3C5 algorithm.
- Contribution of break-up process is considered.
- Applied to elastic scattering by Deuteron incident on target ranging from ^{12}C to ^{208}Pb

Deuteron elastic angular distribution

Compared to
Spherical Optical
Model calc. with
global potential



Deuteron elastic angular distribution



Application to elastic scattering for stable and unstable nuclei

1. ${}^6\text{He}$ incident on ${}^{12}\text{C}$, ${}^9\text{Be}$, ${}^{208}\text{Pb}$, ${}^{209}\text{Bi}$
22.5 – 229.8 MeV

